

Palaeoenvironmental and palaeoclimatic reconstruction of the Witbank coal deposits (Karoo Basin, South Africa)

By Alexander Thomas Wheeler



Submitted in fulfillment of the requirements for the degree Master of Science in
the Faculty of Natural & Agricultural Sciences, University of Pretoria, Pretoria.

November 2015

I, Alexander Thomas Wheeler, declare that the thesis/dissertation, which I hereby submit for the degree Master of Science at the University of Pretoria, is my own work and has not previously been submitted by me for a degree at this or any other tertiary institution.

SIGNATURE:



DATE: 10 November 2015

Abstract

Coal deposits serve as important archives of palaeoclimate change. Palynomorph assemblages reflect the composition of the parent plant communities which are in turn controlled by the local environment and regional climate. Palynofacies can also be used to further interpret the depositional environment and transport mechanisms.

In Main Karoo Basin, the Permian Ecca Group hosts economically important coal deposits within the Witbank and Highveld Coalfields. The most significant deposits are located in the Artinskian/Kungurian-aged No. 2 Coal Seam. The post-glacial fluvio-deltaic deposits represent an important shift in climate in the early Permian. Palynological samples from boreholes of the Witbank Coalfield were analyzed to reconstruct the palaeoenvironment and palaeoclimate signature recorded in palynomorph assemblages and palynofacies patterns of the No. 2 Coal Seam. For comparison additional samples from boreholes of the adjacent Highveld Coalfield were analyzed with respect to distinguish between local and regional signatures. The No. 2 Coal Seam is divided into an Upper Coal Seam and a Lower Coal Seam by a sandstone/siltstone marker bed but this does not extend laterally across the full extent of both basins.

The palaeoenvironment is generally swamp-dominated in the Lower Coal Seam but fluctuates between swamp-dominated and lake/pond-dominated in the Upper Coal Seam. There are differences on a local scale which are controlled by the climate and topography. The palynofacies and intraseam partings in the Witbank Coalfield indicate a highly proximal depositional environment and a more distal depositional environment in the Highveld Coalfield.

The vegetation in the Lower Coal Seam is dominated by conifers in the upland and ferns in the lowland with *Cordaites* occupying the higher valleys. In the Upper Coal Seam the Carboniferous/Permian vegetation is replaced by a more diverse *glossopteris-gangamopteris*-dominated flora.

The climate signal as indicated by the pollen-producing plants is a shift from a stable cold climate in the Lower Coal Seam to a fluctuating cool-temperate climate in the Upper Coal Seam. This change in the climate is caused by the movement of Gondwana northwards and away from the South Pole during the Permian.

Acknowledgements

Firstly, I would like to thank the DST-NRF Centre of Excellence for Integrated Mineral and Energy Resource Analysis sponsoring my research and providing funding to present my work overseas. I would also like to thank AASP for the travel grant which helped cover my travel costs.

I am deeply grateful to my supervisor, Professor Annette Götz for tireless support and assistance in the completion of this project and constantly pushing to make sure I had the financial and institutional support I would need to complete my research.

I would like to extend a big thank you to Dr. Nils Lenhardt for advice and assistance while completing my research. I would also like to thank him, Sukanya Lenhardt and Gert-Jan Peeters for the great food, conversation and games which made my time in Pretoria a lot more enjoyable.

Lastly, I would like to thank my family, particularly my parents, for their love and support. It is thanks to them that I am lucky enough to be able to pursue a career in the field of my choosing.

Table of Contents

Abstract

Acknowledgements

1. Introduction	1
1.1 Motivation	1
1.2 Aims	1
1.3 Palynofacies	2
1.4 Previous Work	2
2. Geological Setting	6
2.1 Main Karoo Basin	6
2.2 Stratigraphy	7
2.2.1 Dwyka	7
2.2.2 Ecca	7
2.2.2.1 Vryheid Formation	8
2.2.3 Beaufort	11
2.2.4 Stormberg	11
2.3 Coalfields of South Africa	11
2.3.1 Witbank and Highveld Coalfields	13
2.3.2 Waterberg Coalfield	17
2.3.3 Other Coalfields	17
3. Materials and Methods	18
3.1 Samples	18
3.2 Palynological Processing	19
3.3 Classification of Particulate Organic Matter	20
3.3.1 Phytoclasts	21

3.3.2	Sporomorphs	21
3.3.3	Degraded Organic Matter (DOM) and Amorphous Organic Matter (AOM)	22
3.3.4	Algae	22
3.4	Palynofacies Analysis	22
4.	Results	25
4.1	Description of Samples	25
4.1.1	Palesa	25
4.1.2	HWH1418	29
4.1.3	BHS14	34
4.1.4	ALBN11	38
4.1.5	K114134	43
4.1.6	S542145	48
5.	Discussion	53
5.1	Palaeoenvironment Analysis	53
5.2	Vegetation	55
5.2.1	Lower Coal Seam	55
5.2.2	Upper Coal Seam	57
5.3	Palaeoclimate Analysis	59
5.4	Comparison of Lower and Upper Coal Seam	60
5.5	Comparison of Witbank and Highveld Coalfields	60
6.	Conclusions	63
7.	Outlook.....	64
	References.....	65
	Appendices.....	i

- **Palynofacies Counting Sheets** **i**
- **Photo Plates** **ii**

List of Figures

Figure 1.1: Correlation of international chronostratigraphic units with palynostratigraphic biozones based on South African localities (adapted from MacRae & Aitken, 1997).	4
Figure 1.2: Climate reconstruction of the Main Karoo Basin based on pollen-producing flora (From Hancox & Götz, 2014, modified after Falcon, 1986).	5
Figure 2.1: Carboniferous-Permian-Triassic foreland basins which formed in southern Gondwana (from Hancox & Götz, 2014).	6
Figure 2.2: Distribution of the four main stratigraphic groups of the Main Karoo Basin and the location of this study marked in red (from Catuneanu <i>et al.</i> , 2002).	8
Figure 2.3: Correlation of the Whitehill Formation with the No. 5 Coal Seam of the Vryheid Formation based on palynological evidence (from Hancox & Götz, 2014).	9
Figure 2.4: Correlation of the Vryheid Formation with the Whitehill Formation based on proximal and distal facies development (Johnson <i>et al.</i> , 1996) or with the Ripon Formation based on sequence stratigraphy (Catuneanu <i>et al.</i> , 2002).	10
Figure 2.5: Correlation of the Vryheid Formation with the Ripon Formation using sequence stratigraphy (Catuneanu <i>et al.</i> , 2002).	10
Figure 2.6: Distribution of the 19 major coalfields in South Africa (adapted from Fourie <i>et al.</i> , 2014).	12
Figure 2.7: Generalised stratigraphy of the Witbank Coalfield and positions of the five main coal seams (from Hancox & Götz, 2014).	14
Figure 2.8: Lateral extent of siltstone and sandstone partings in the No. 2 Coal Seam (from Hancox & Götz, 2014).	15

Figure 2.9: Generalised stratigraphy of the Highveld Coalfield and the positions of the six main coal seams (from Hancox & Götz, 2014). **16**

Figure 3.1: Map showing the extent of the Vryheid Formation as well as surface outcrops of Jurassic dolerite intrusions. Sampling locations in the Witbank and Highveld coalfields are marked by red dots. Used abbreviation in key: Fm=Formation (based on Department of Mineral and Energy Affairs, 1986; Based on Department of Mines, 1978). **19**

Figure 3.2: Classification of particulate organic matter and preservation potential of each category (Götz & Ruckwied, 2014). **20**

Figure 3.3: Phytoclast palynofacies parameters used for palaeoenvironment interpretation and reconstruction (from Tyson, 1995). **24**

Figure 4.1: Spindle diagram showing relative abundance of sporomorphs, AOM, DOM and freshwater algae at Palesa locality. AOM – amorphous organic matter, DOM – degraded organic matter. **26**

Figure 4.2: Spindle diagram showing relative abundances of phytoclasts at Palesa locality. **27**

Figure 4.3: Graph showing spore:pollen, opaque:translucent phytoclast and equidimensional:blade-shaped phytoclast ratios at Palesa locality. **28**

Figure 4.4: Spindle diagram showing relative abundances of sporomorphs, AOM, DOM and freshwater algae at HWH1418 locality. AOM – amorphous organic matter, DOM – degraded organic matter. **31**

Figure 4.5: Spindle diagram showing relative abundances of phytoclasts at HWH1418 locality. **32**

Figure 4.6: Graph showing spore:pollen, opaque:translucent phytoclast and equidimensional:blade-shaped phytoclast ratios at HWH1418 locality. **33**

Figure 4.7: Spindle diagram showing relative abundances of sporomorphs, AOM, DOM and freshwater algae at BHS14 locality. AOM – amorphous organic matter, DOM – degraded organic matter.	35
Figure 4.8: Spindle diagram showing relative abundance of phytoclasts at BHS14 locality.	36
Figure 4.9: Graph showing spore:pollen, opaque:translucent phytoclast and equidimensional:blade-shaped phytoclast ratios at BHS14 locality.	37
Figure 4.10: Spindle diagram showing relative abundances of sporomorphs, AOM, DOM and freshwater algae at ALBN11 locality. AOM – amorphous organic matter, DOM – degraded organic matter.	40
Figure 4.11: Spindle diagram showing relative abundances of phytoclasts at ALBN11 locality. ...	41
Figure 4.12: Graph showing spore:pollen, opaque:translucent phytoclast and equidimensional:blade-shaped phytoclast ratios at ALBN11 locality.	42
Figure 4.13: Spindle diagram showing relative abundances of sporomorphs, AOM, DOM and freshwater algae at K114134 locality. AOM – amorphous organic matter, DOM – degraded organic matter.	45
Figure 4.14: Spindle diagram showing relative abundances of phytoclasts at K114134 locality.	46
Figure 4.15: Graph showing spore:pollen, opaque:translucent phytoclast and equidimensional:blade-shaped phytoclast ratios at K114314 locality.	47
Figure 4.16: Spindle diagram showing relative abundances of sporomorphs, AOM, DOM and freshwater algae at S542145 locality. AOM – amorphous organic matter, DOM – degraded organic matter.	50
Figure 4.17: Spindle diagram showing relative abundances of phytoclasts at S542145 locality.	51
Figure 4.18: Graph showing spore:pollen, opaque:translucent phytoclast and equidimensional:blade-shaped phytoclast ratios at S542145 locality.	52

Figure 5.1: Palaeotopographic reconstruction of the central Witbank Coalfield and possible routes of river channels (adapted from Falcon, 1989).54

Figure 5.2: Model of the environment and vegetation of the Lower Coal Seam of the Witbank Coalfield and adjacent Highveld Coalfield. Small plants represent ferns, horsetail ferns and lycopods. Light green trees represent *Cordaites* flora. Dark green trees represent upland conifers. Red markers indicate studied localities.56

Figure 5.3: Model of the environment and vegetation of the Upper Coal Seam of the Witbank Coalfield. Small plants represent cycads, ferns and horsetail ferns. Light green trees represent Glossopterid flora. Dark green trees represent upland gymnosperms. Red markers indicate studied localities.58

Figure 5.4: Map of the five major valleys in the Witbank Coalfield (From Hancox & Götz, 2014).61

Figure 7.1: Schematic diagram of the Sporomorph EcoGroup Model. Plant species are grouped into different SEGs based on their habitat preferences which are controlled by the climate and environment (adapted from Abbink, 2001).64

1. Introduction

1.1 Motivation

The near-continuous deposition of sediments in the Main Karoo Basin in South Africa from the late Carboniferous to the mid-Jurassic captures an extensive period of climate change from a glacial through to a dry arid climate (Falcon *et al.*, 1984). The coal deposits of the Witbank Coalfield and more specifically the No. 2 Coal Seam captures a crucial climatic shift in the Permian. As glaciers receded, the climate and environment supported the development of peat-forming wetlands in the north-eastern part of the Main Karoo Basin. In areas with such well-developed floral assemblages one of the best methods of reconstructing the palaeoclimate and palaeoenvironment is palynology. A palynological assemblage reflects its parent plant community which in turn is controlled by the climatic and environmental conditions (Gastaldo, 1994). This makes it a powerful tool to look at changes in the climate and environment on high time resolution at multiple localities. It also allows for the development of new methods of correlating the South African coalfields for exploration of potential remaining coal resources in the northern part of the country which is especially important in light of the current energy crisis affecting South Africa.

1.2 Aims

The aim of this study is to use palynological samples from multiple localities in the Witbank Coalfield as well as from the adjacent Highveld Coalfield to reconstruct the palaeoclimate history and to observe changes in the local palaeoenvironment at each locality. This will allow one to identify both local conditions which are specific to different parts of the basin as well as regional signatures. Another aim of the study is to use the palynofacies and climate signal to see if one can differentiate between the Lower and Upper coal seams which make up the No. 2 Coal Seam even when an intraseam parting is not present. This will further develop the utilization of palynofacies as a tool to stratigraphic correlation even within a single coal seam.

1.3 Palynofacies

The term palynofacies is used to refer to an assemblage of acid-resistant organic material which reflects a specific sedimentary environment (Powell *et al.*, 1990) or an organic facies defined by the palynological composition (Tyson, 1995). This includes sporomorphs (pollen and spores) as well as plant debris in the form of phytoclasts. By analyzing both the palynomorphs and palynodebris collectively one can gain further insight into both the parent plant assemblage as well as the depositional environment (Gastaldo, 1994; Traverse, 2007). The palynodebris displays similar effects during transportation as sedimentary particles, in terms of sorting and rounding, and can thus be used to interpret the manner and energy of transport (Traverse, 2007).

1.4 Previous Work

Hart (1967) developed the first biozonation scheme based on palynology in the Main Karoo Basin (Fig. 1.1). Four zones were defined for the Permian and Carboniferous strata but their relatively wide time range limited their application to basin-wide correlation (MacRae & Aitken, 1997).

Anderson (1977) completed the most comprehensive palynological study done for the Permian in South Africa. The study describes and maps the distribution of a large variety of palynomorphs as well as suggesting botanical affinities for many of the sporomorphs studied. The study also includes a detailed biozonation scheme using palynomorphs which can be applied to the Main Karoo Basin consisting of eight zones and twenty one subzones. Subsequent studies which attempt interbasinal correlation of the Main Karoo Basin with coeval basins in other parts of Gondwana use this scheme for biostratigraphic comparison (Backhouse, 1991; Stephenson & McClean, 1999; Stephenson, 2008).

Falcon *et al.* (1984) used palynological and sedimentological samples from the Witbank Coalfield to begin determining the environmental and climatic history of the basin (Fig. 1.2) as well as to develop a biozonation scheme based on palynological assemblages. The data studied

here forms the basis of the current idea of Permian post-glacial climate amelioration which Falcon (1986) proposed as occurring as a series of smaller ice ages as opposed to a continuous event.

MacRae (1988) studied the palynology of the Waterberg and Parfuri basins and set up six palynostratigraphic zones which he used to correlate these basins with other coeval basins.

Work was done on the No. 5 Coal Seam in the Witbank Coalfield by Aitken (1993, 1994). This work catalogues the palynomorphs found in the coal seam as well as attempts to correlate the seam with other parts of the Main Karoo Basin. This paper also outlines the possible environment in which the coals formed based on the palynomorph assemblage and previous work by Falcon (1986). Further work was done to develop a biostratigraphic zonation scheme for the northern part of the Main Karoo Basin as well as further interpret the palaeoenvironment (Aitken, 1998).

Millstead (1994, 1999) did palynological work on samples from the Orange Free State Coalfield with the intention of getting a more accurate age for the coal deposits through correlation with the Witbank and Highveld coalfields.

Since then, not much palynological work has been completed in South Africa until Barbolini (2010, 2014) who attempted to correlate the palynostratigraphy of the Main Karoo Basin with other Karoo-aged basins in Africa and the rest of Gondwana. Significant work was done by Götz & Ruckwied (2014) in the No. 2 Coal Seam of the Witbank Coalfield in terms of using palynofacies to create a high resolution image of the palaeoenvironment and palaeoclimate based on the climate signal inferred by Falcon (1986). Ruckwied *et al.* (2014) used the climate signal inferred from the Witbank Coalfield in order to correlate the Whitehill Formation with the biozones from Falcon *et al.* (1984) and the No. 5 Coal Seam from the Witbank Coalfield in the Vryheid Formation.

Chronostratigraphic Units				South Africa						
				N. Karoo Basin	Waterberg/Pafuri	Main Basin	Main Karoo Basin	North Main		
Period	Epoch	Age	Chron	Aitken 1998	MacRae 1988	Hart 1967	Anderson 1977	Falcon 1978		
Triassic	Early Triassic	Scythian		X						
				IX						
Permian	Late Permian	Tartarian		VIII	F	Striatiti Zone	Zone 7			
				VII					Zone 6	
				VI						Zone 5
				V					Zone 4	
		IVB		IV			h			
		IVA						E	Zonati Zone	d
	Early Permian	Kungurian	Irenian	III	D	Cingulati Zone	Zone 3 b			
			Filpovian							
		Artinskian	Baigendzinian	II				d	II	e
			Aktaskian							
		Sakmarian	Sterlitamakian	I	B	Cavati Zone	Zone 2 c	b	c	
										Tastubian
Asselian	Krumaian		a					I		b
	Uskalikian									
Surenan										
Carboniferous	Gzelian	Noginskian	Dwyka	A	Zone 1	a				
		Klazminskian								
		Dorogomilovskian								
	Kasimovian									

Figure 1.1: Correlation of international chronostratigraphic units with palynostratigraphic biozones based on South African localities (adapted from MacRae & Aitken, 1997).

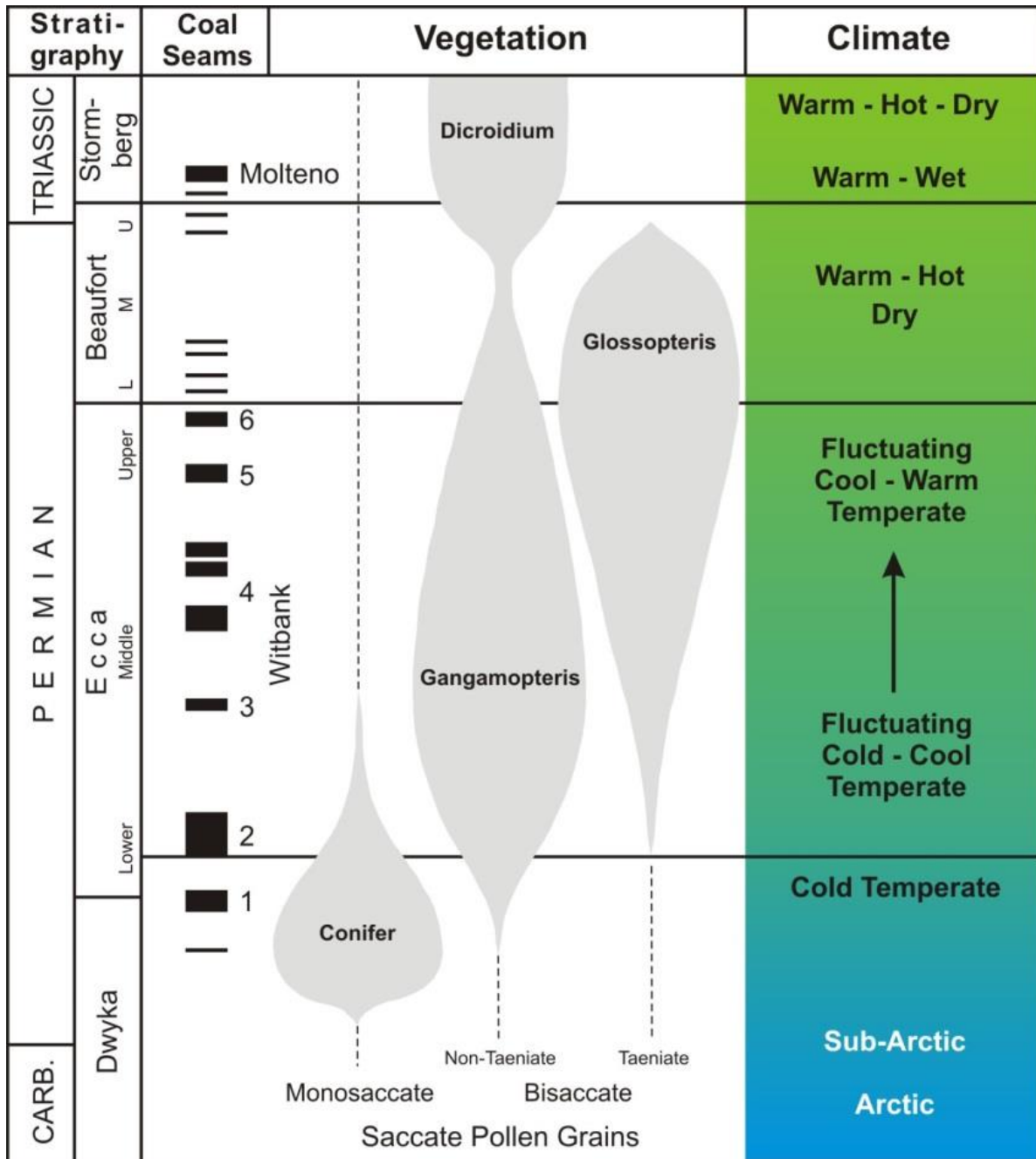


Figure 1.2: Climate reconstruction of the Main Karoo Basin based on pollen-producing flora (From Hancox & Götz, 2014; modified after Falcon, 1986).

2. Geological Setting

2.1 Main Karoo Basin

The Main Karoo Basin is a retroarc foreland basin which formed north of the Cape Fold Belt and is part of a series of other Gondwanan basins which formed between the Late Palaeozoic to Early Mesozoic (Catuneanu *et al.*, 2005) (Fig. 2.1). The basin was bound to the north by the Cargonian Highlands and to the south by the Cape Fold Belt (Isbell *et al.*, 2008). The sedimentary sequence which fills the Main Karoo Basin is known as the Karoo Supergroup and is split into four main groups (Dwyka, Ecca, Beaufort, Stormberg) which were deposited over the course of approximately 120 million years from the Late Carboniferous to the Middle Jurassic and terminated with the eruption of the Drakensberg basaltic lavas (Fig. 2.2). Jurassic-aged igneous intrusions (dykes and sills) associated with the volcanism are common in the Main Karoo Basin (Cadle *et al.*, 1993). These intrusions caused local metamorphism in the northern part of the basin producing meta-anthracites and may be responsible for destroying oil and gas deposits in the south (Cadle *et al.*, 1993).

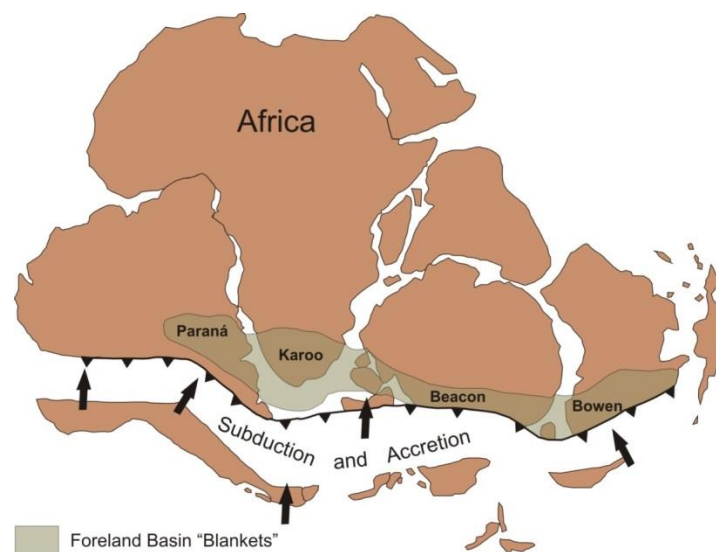


Figure 2.1: Carboniferous-Permian-Triassic foreland basins which formed in southern Gondwana (from Hancox & Götz, 2014).

2.2. Stratigraphy

2.2.1 Dwyka

The Dwyka Group (Fig. 2.2, 2.3, 2.4) represents the first depositional sequence in the Main Karoo Basin in the Carboniferous. The main rock types associated with the group are diamictites, tillites and fluvioglacial sandstones and conglomerates which indicate a glacial depositional environment (Johnson *et al.*, 1996). Deposition ceased when climate amelioration caused large-scale deglaciation in the Main Karoo Basin (Falcon, 1986).

2.2.2 Ecca

The sixteen formations that make up the Ecca Group represent the majority of Permian-aged deposits in the Main Karoo Basin (Johnson *et al.*, 1996). In the southern part of the basin (Fig. 2.4) the sequence is comprised mainly of mudrock, black shales and sandstone. The lowermost Prince Albert Formation also features shallow water carbonates while the overlying Whitehill Formation features organic-rich black shales. These black shales have been identified as the target for future exploration for possible shale gas extraction in South Africa. The Collingham Formation is made up siliceous mudrock interbedded with ashfall tuff beds associated with arc volcanism to the south (McKay *et al.*, 2015). The turbiditic sandstones of the Ripon, Laingsburg and Skoorsteenberg formations represent submarine fan complexes deposited on the slope (Johnson *et al.*, 1996; Johnson *et al.*, 2001; Hodgson *et al.*, 2006; Flint *et al.*, 2010).

There is a significant lateral shift in the depositional environment towards the north-eastern part of the basin. This area is comprised of three distinct formations (Fig. 2.4): the shales of the Pietermaritzburg Formation, cyclic fluvio-deltaic siliciclastics and coal deposits of the Vryheid Formation and the siltstone and mudstone deposits of the Volksrust Formation (Hancox & Götz, 2014).

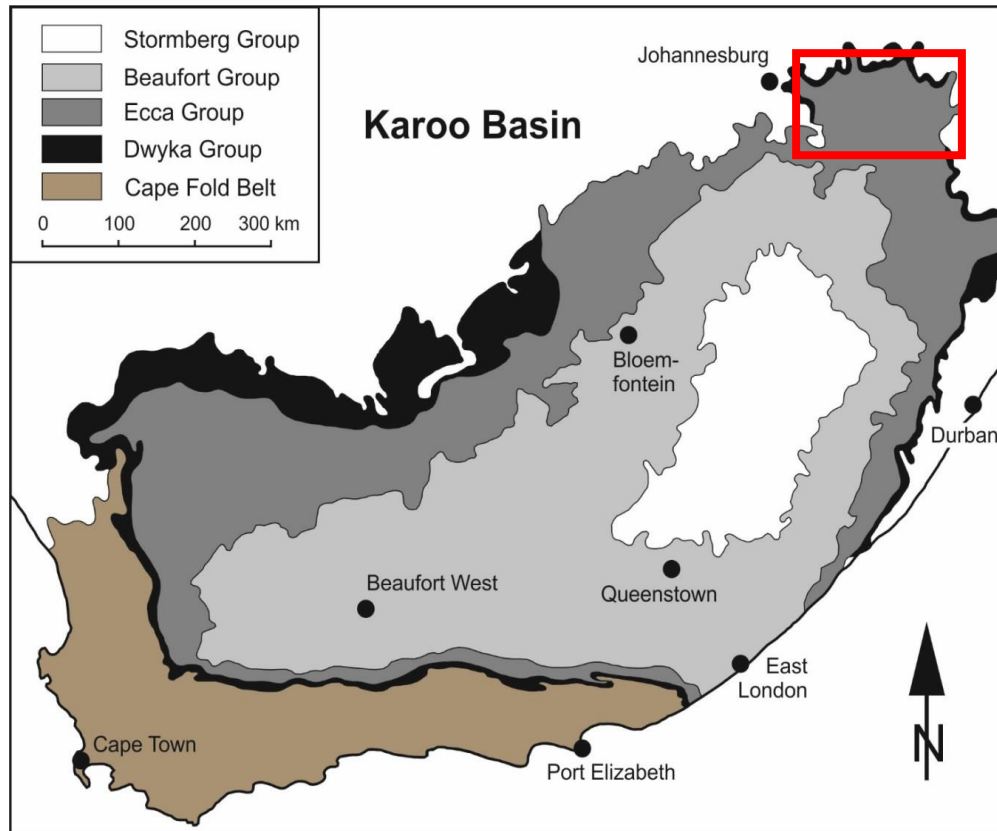


Figure 2.2: Distribution of the four main stratigraphic groups (Dwyka, Ecca, Beaufort, Stormberg) of the Main Karoo Basin and the location of this study marked in red (from Catuneanu *et al.*, 2002).

2.2.2.1 Vryheid Formation

The Vryheid Formation represents an extensive peat-forming environment that formed around the coast of the Karoo Sea (Cadle *et al.*, 1993). Deposition appears to have occurred in at least five upward-coarsening deltaic sequences and upward-fining fluvial sequences which terminate with a layer of coal (Johnson *et al.*, 1997). As shown in Figure 2.3, palynological evidence suggests that the Whitehill Formation correlates with No. 5 Coal Seam of the Witbank Coalfield (Götz, 2014; Ruckwied *et al.*, 2014). This interpretation is also suggested by Johnson *et al.*, (1996) as well as Catuneanu *et al.* (1998) (Fig. 2.4) when comparing the proximal and distal facies of the Ecca Formation as the Karoo Foreland Basin developed. However, Catuneanu *et al.* (2002) used a sequence stratigraphic approach to correlate the five major cyclic depositional

patterns in the Vryheid Formation with the five stacked sequences of submarine fans of the Ripon Formation (Fig. 2.5). The Cargonian Highlands formed the main source of sediment to the northern part of the Main Karoo Basin and remained glaciated during deposition of the Vryheid Formation (Isbell *et al.*, 2008).

S Karoo Götz & Ruckwied (2014)	N Karoo Ruckwied et al. (2014)	Biozones Falcon et al. (1984)	NE Karoo (Witbank)	
Collingham Fm.	Tierberg Fm.	IV	h ¹ Coal Seam No. 6	
Whitehill Fm.	Whitehill Fm.		h Coal Seam No. 5	
Prince Albert Fm.	Prince Albert Fm.	III	f Coal Seam No. 4	
			II	e Coal Seam No. 3
				d Coal Seam No. 2
?	?	I	c Coal Seam No. 1	
			b	
		a		
			Pieter-maritzburg Fm.	
Dwyka Group				

Figure 2.3: Correlation of the Whitehill Formation with the No. 5 Coal Seam of the Vryheid Formation based on palynological evidence (from Hancox & Götz, 2014).

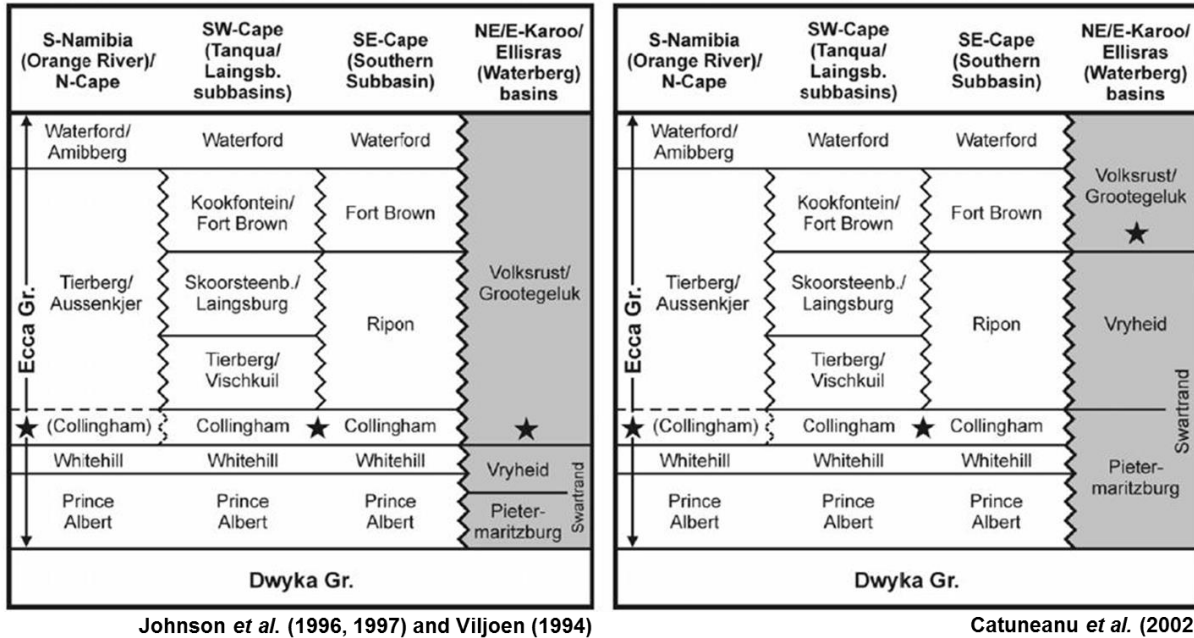


Figure 2.4: Correlation of the Vryheid Formation with the Whitehill Formation based on proximal and distal facies development (Johnson *et al.*, 1996) or with the Ripon Formation based on sequence stratigraphy (Catuneanu *et al.*, 2002)

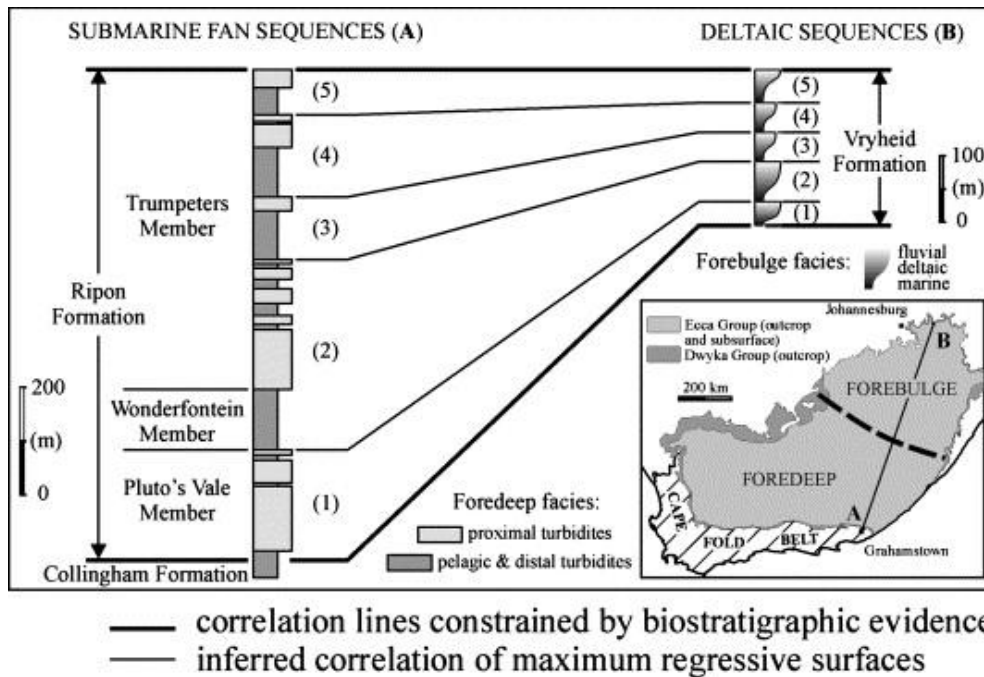


Figure 2.5: Correlation of the Vryheid Formation with the Ripon Formation using sequence stratigraphy (Catuneanu *et al.*, 2002).

2.2.3 Beaufort

The Beaufort Group is a terrestrial sequence of fluvio-deltaic sandstones and mudstones as well as conglomerates and granulestones. This group has incredible significance as it features one of the most complete records of therapsid remains in the world, which has allowed for the development of a biostratigraphic zonation scheme based on the distribution of these fossils (Broom, 1906; Rubidge *et al.*, 1995). The P-T boundary is also thought to be located within this group based on the disappearance of many major therapsid groups from the fossil record and recent zircon data obtained from localities in the Eastern Cape (Rubidge *et al.*, 2013).

2.2.4 Stormberg

The Late Triassic to Mid-Jurassic Stormberg Group is the uppermost unit of the Karoo Supergroup and is capped by the Drakensberg Group basalts (Catuneanu *et al.*, 2005). The three sedimentary formations appear to indicate a climate that is become increasingly arid (Johnson *et al.*, 1997). The fluvial sandstones of the Molteno Formation are overlain by fine-grained sandstones and mudstones of a fluvial and floodplain dominated Elliot Formation. The arid aeolian sandstones of the Clarens Formation were the last sediments deposited before the eruption of the Drakensberg lavas (Johnson *et al.*, 1997).

2.3 Coalfields of South Africa

Coal is an incredibly important source of energy in South Africa. Currently around 77% of the country's electricity is produced by coal-fired power stations while the remainder is produced mainly by smaller hydroelectric, the Koeberg nuclear power station (Eskom, 2015). Projects involving renewable wind and solar energy are now being implemented at a larger scale but for the foreseeable future coal will remain South Africa's primary means of generating electricity (Eskom, 2015). This makes it important to understand the coalfields currently being exploited as well as potential new resources. It is generally accepted that there are 19 distinct coalfields in South Africa though only around six or seven have been used for coal production (Hancox & Götz, 2014) (Fig. 2.6). The most intensely exploited and researched are the Witbank and

Highveld coalfields but the Waterberg coalfield has been identified as a potential replacement once their economically viable deposits are depleted (Hancox & Götz, 2014).



Figure 2.6: Distribution of the 19 major coalfields in South Africa (adapted from Fourie *et al.*, 2014).

2.3.1 Witbank and Highveld Coalfields

The Witbank Coalfield is regarded as the one of the most economically important coal resources in South Africa currently being exploited (Snyman, 1998; Hancox & Götz, 2014). The sedimentary fill of the Witbank Coalfield is mainly made up of the fluvio-deltaic Vryheid Formation which sits on either the pre-Karoo basement or Dwyka tillites (Cairncross, 1989). The coal deposits of the Witbank Coalfield (Fig. 2.7) are separated by interseam partings of sandstone or siltstone as well as intraseam partings (Fig. 2.8). These partings do not continue laterally throughout the whole coalfield and pinch out towards the south and east (Cairncross & Cadle, 1988). The coals of the Witbank Coalfield are ranked as high volatile bituminous coals (Falcon, 1986). The No. 2 Coal Seam, the main target seam for mining, is the thickest coal seam in the coalfield averaging around 4-5m, although varying intraseam parting thickness can push thickness as high as 40m and as low as 2m (Cairncross & Cadle, 1988). The No. 2 Coal Seam is divided into an Upper Coal Seam (2U) and a Lower Coal Seam (2L) (Fig. 2.8) with both seams yielding a high inertinite content and variable fusinite and vitrinite contents (Cadle *et al.*, 1993).

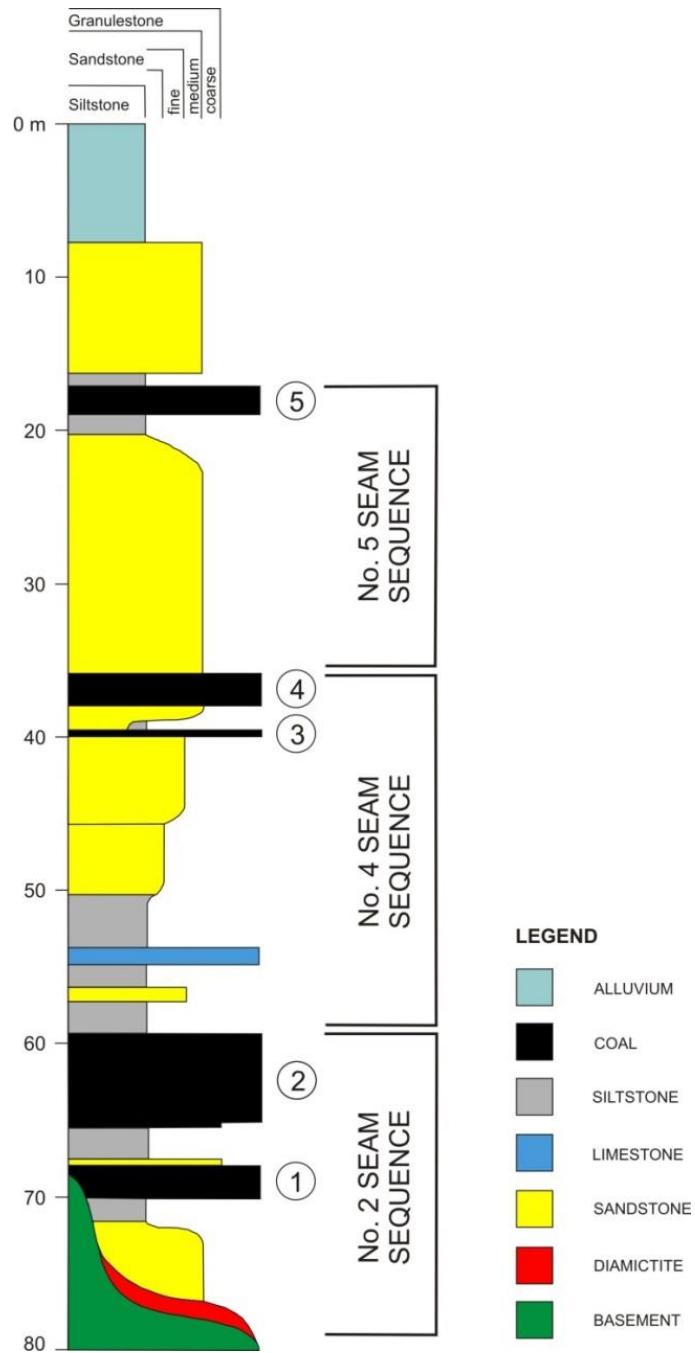


Figure 2.7: Generalised stratigraphy of the Witbank Coalfield and positions of the five main coal seams (from Hancox & Götzt, 2014).

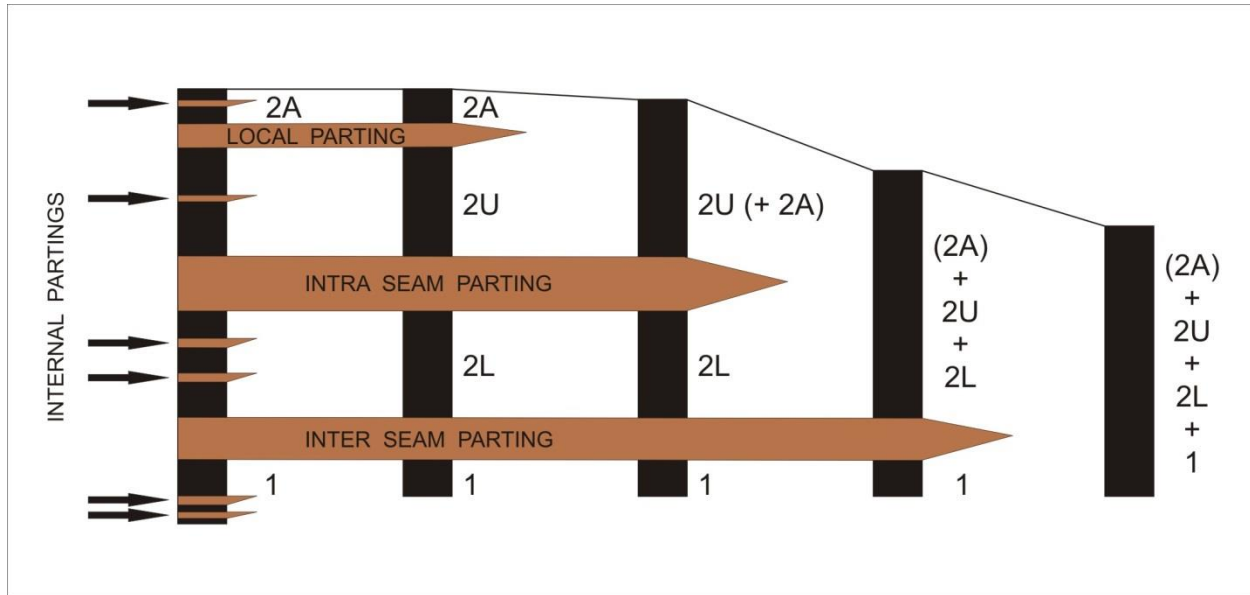


Figure 2.8: Lateral extent of siltstone and sandstone partings in the No. 2 Coal Seam (from Hancox & Götz, 2014).

The Highveld Coalfield is separated from the Witbank Coalfield by an outcrop of basement known as the Smithfield Ridge which formed a topographical palaeohigh during the deposition of Vryheid Formation sediments (Hancox & Götz, 2014). The No. 2 Coal Seam in the Witbank Coalfield is separated from that of the Highveld Coalfield's equivalent unit by the palaeohigh, but the No. 4 Coal Seam extends over the top (Cairncross, 1989). The stratigraphy of the Highveld Coalfield (Fig. 2.9) greatly resembles that of the Witbank Coalfield (Fig. 2.7) because they were deposited in very similar environments coevally. Variability in the coals themselves is caused by differences in palaeovalleys on either side of the ridge as well as differential compaction of the coal running over the top, but maintains a similar rank as a high volatile bituminous coal (Cairncross, 1989; Falcon, 1986).

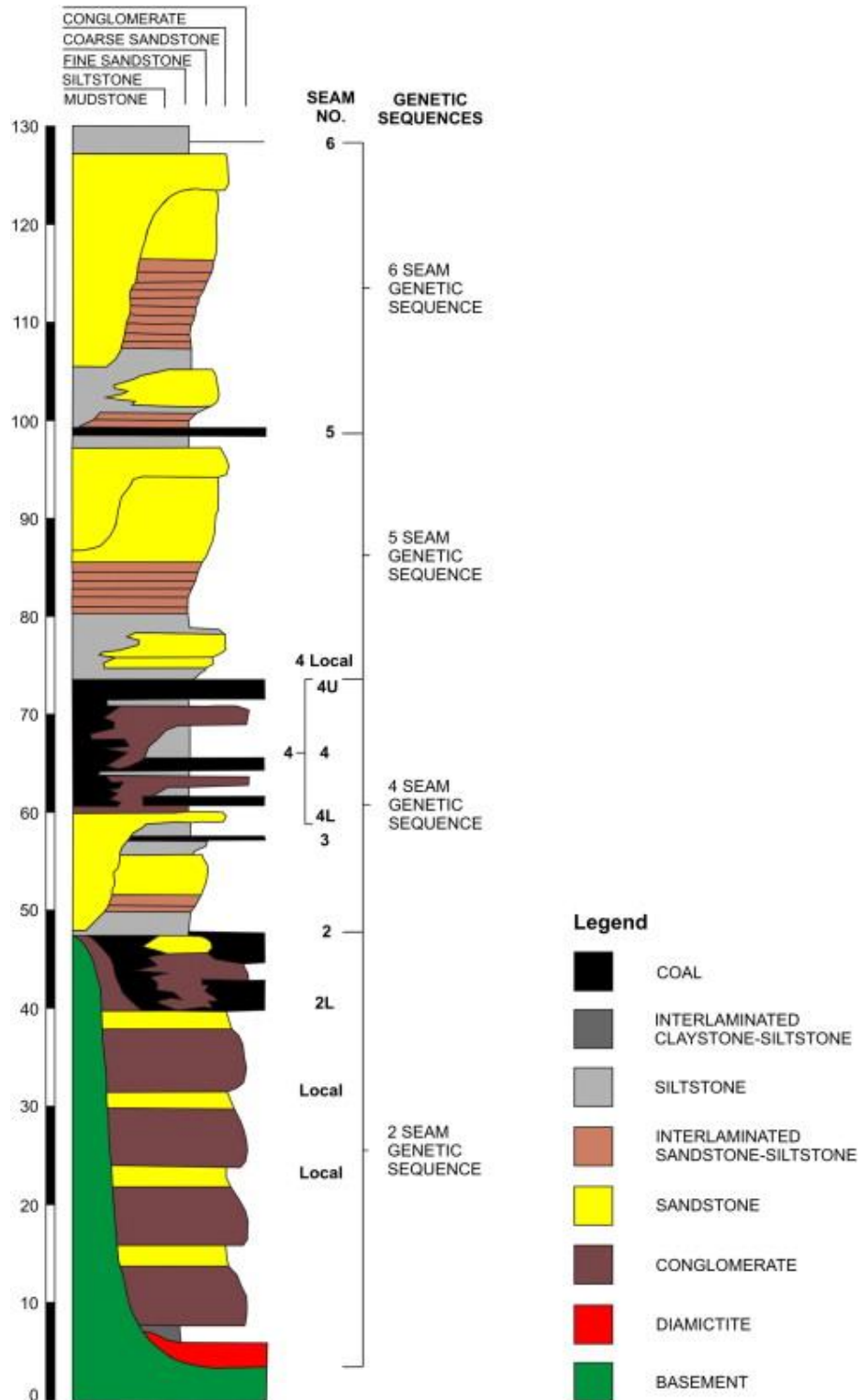


Figure 2.9: Generalised stratigraphy of the Highveld Coalfield and the positions of the six main coal seams (from Hancox & Götz, 2014).

2.3.2 Waterberg Coalfield

The Waterberg Coalfield in the Ellisras Basin (Fig. 2.6) has been identified as a valuable potential coal resource which will take over from the Witbank and Highveld Coalfields as South Africa's most important coal producing basin later in the 21st century (Fourie *et al.*, 2014). The eleven coal zones occur in both the Vryheid Formation (zones 1 to 4) and the overlying Grootgeluk Formation (zones 5 to 11). The coal from the Vryheid Formation has mainly been identified as dull coal while the Grootgeluk Formation yields bright coals intercalated with organic-rich mudstones. Mining in the Waterberg Coalfield has been complicated by the presence of numerous faults. Recent research has focused on seeing how the major fault zones (Eenzaamheid, Daarby, Zoetfontein) and numerous smaller faults have affected the coal deposits (Fourie *et al.*, 2014). Future mining may need to continue underground to access the potential resources of the Waterberg Coalfield.

2.3.3 Other Coalfields

The Ermelo Coalfield lies adjacent to the Witbank and Highveld coalfields (Fig. 2.6). The coals are of similar quality but the seams are thinner and pinch out in places (Hancox & Götz, 2014). There is also more structural complexity which makes it a less favourable target for mining compared to the Witbank and Highveld Coalfields, but it has nonetheless seen substantial development due to its proximity to the transport route to the port in Richards Bay (Hancox & Götz, 2014).

In KwaZulu-Natal, the Vryheid, Utrecht and Kliprivier coalfields are associated with the Main Karoo Basin (Fig. 2.6), while the younger Nongoma and Somkhele coalfields formed through processes related to the rifting of Gondwana (Hancox & Götz, 2014).

The Free State Coalfield is the biggest coalfield in the country (Fig. 2.6) but has seen little development since the best target seams lie at a depth of 350-450m, which would require underground mining to reach (Hancox & Götz, 2014). Macrofossil evidence correlates the coal deposits with the Vryheid Formation (Millstead, 1994).

3. Materials and Methods

3.1 Samples

Core samples of the No. 2 Coal Seam were collected from four drill sites in the Witbank Coalfield and two drill sites in the Highveld Coalfield (Fig. 3.1). Samples represent organic-rich siltstones from the Lower and Upper Seam and intraseam sand- and siltstones. Samples were processed at Paly Parlour Laboratory in the United Kingdom.

10 samples were collected from the northern part of the Witbank Coalfield at location Palesa (25°32'01.40" S, 028°46'12.82" E). Samples were collected from siltstones at regular intervals as no intraseam parting was present.

14 samples were collected in the central-eastern part of the Witbank Coalfield at location HWH1418 (25°57'02.68" S, 029°26'36.85" E). 4 samples were collected from the Lower Coal Seam, 3 were collected from the intraseam parting and 7 were collected from the Upper Coal Seam.

10 samples were collected in the central-western part of the Witbank Coalfield at location BHS14 (26°04'05.00" S, 029°00'43.00" E). Samples were collected from siltstones at regular intervals as no intraseam parting was present.

8 samples were collected in the southern part of the Witbank Coalfield at location ALBN11 (26°08'39.41" S, 029°18'15.85" E). 3 samples were collected from the Lower Coal Seam, 1 was collected from the intraseam parting and 4 were collected from the Upper Coal Seam.

12 samples were collected in the northern part of the Highveld Coalfield at location K114134 (26°23'30.30" S, 029° 17'14.10" E). 5 samples were collected from the Lower Coal Seam, 2 were collected from the intraseam parting and 5 were collected from the Upper Coal Seam.

8 samples were collected in the central-western part of the Highveld Coalfield at location S542145 (26° 37'46.13" S, 028° 51'19.72" E). 3 samples were collected from the Lower Coal Seam, 1 was collected from the intraseam parting and 4 were collected from the Upper Coal Seam.

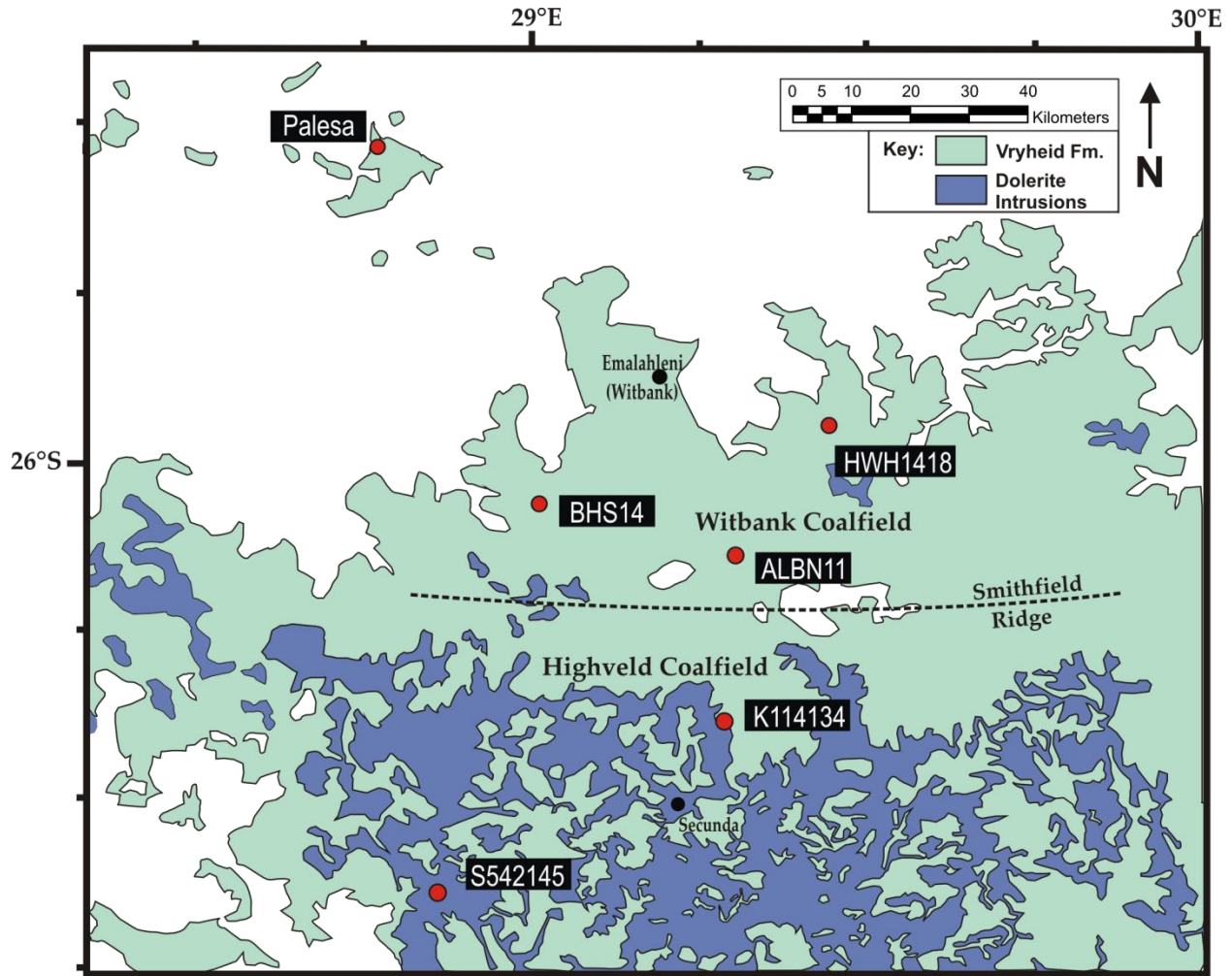


Figure 3.1: Map showing the extent of the Vryheid Formation as well as surface outcrops of Jurassic dolerite intrusions. Sampling locations in the Witbank and Highveld coalfields are marked by red dots. Used abbreviation in key: Fm. = Formation (based on Department of Mines, 1978; Department of Mineral and Energy Affairs, 1986).

3.2 Palynological Processing

All 62 samples were prepared using standard palynological processing techniques as described in Vidal (1988) though with higher concentrations of acids to account for the high mineral content. The samples were treated with a 33% HCl solution and a 73% HF solution to dissolve carbonates and silicates. Density separation was done using a saturated ZnCl₂ solution. The residues were then sieved through a 15µm mesh and mounted on slides using the mounting medium Eukitt.

3.3 Classification of Particulate Organic Matter

Counts of between 500 and 600 were done for each of the 62 samples collected for a statistically viable dataset and classified based on the scheme used in Götz & Ruckwied (2014) (Fig. 3.2). This scheme divides the material into categories based on the original material and preservation potential.

Origin	Group	Constituent	preservation potential	
			low	high
higher plant debris	phytoclasts	opaque phytoclasts		██████████
		translucent phytoclasts		██████████
pollen	sporomorphs	pollen grains	██████████	
spores		spores	██████████	
degraded plant debris	degraded organic matter amorphous organic matter		██████████	
degraded algae				
fresh water algae		<i>Tetraporina</i> spp. <i>Botryococcus</i> spp.	██████████	

Figure 3.2: Classification of particulate organic matter and preservation potential of each category (Götz & Ruckwied, 2014).

3.3.1 Phytoclasts

The phytoclasts represent preserved woody material and vascular tissue such as tracheids which have been deposited along with sedimentary particles and sporomorphs (Tyson, 1995). This category also includes cuticular epidermal leaf fragments though the preservation potential is lower due to the fragile nature of the material (Traverse, 2007). The phytoclast category is further divided based on the size, shape and colour of the material. Opaque phytoclasts are highly oxidised and are black in colour. Translucent phytoclasts are yellow to brown in colour. Blade/needle-shaped phytoclasts have a length to breadth ratio of more than 2:1 as opposed to equidimensional phytoclasts which have a length to breadth ratio of less than 2:1.

3.3.2 Sporomorphs

Sporomorphs studied in palynology are the preserved microspore walls of embryophytic plants (Traverse, 2007). These walls chemically consist of sporopollenin which is highly resistant giving the sporomorphs a high preservation potential. Sporomorphs are further divided into pollen grains and spores.

Spores-producing plants require standing bodies of water to reproduce which limits the distance spores can be transported. Classification is based on the size and shape of the spore, the thickness of the exine layer and the texture of the outer surface. Spores are also divided into monolete and trilete spores based on the type of laesurae scars on the surface of the spore.

Permian pollen grains representing gymnosperms have air sacchi attached to them allowing for transport over much greater distances by means of wind. Monosaccate pollen grains have a single air saccus surrounding the grain. Bisaccate pollen grains have two air sacchi attached to the grain. Bisaccate taeniate pollen grains associated with Glossopterids also have striations running across the grain.

3.3.3 Degraded Organic Matter (DOM) and Amorphous Organic Matter (AOM)

Palynomorphs that have been mechanically fragmented during transport are referred to as degraded organic matter (DOM). This material can no longer be classified because the identifying features have been destroyed. River-dominated environments produce high abundances of DOM as palynomorphs are broken up in turbulent water in streams before deposition.

Amorphous Organic Matter (AOM) forms when palynomorphs and phytoclasts degrade chemically. The material becomes structureless and under a transmitted light microscope it appears to have a grainy or clotted "grumose" texture (Tyson, 1995). Since AOM can form from a wide range of organic particles, this group is highly variable. Abundant AOM indicates relatively low oxygen content and high nutrient values in the depositional environment (Traverse, 2007).

3.3.4 Algae

In the case of this study, algal-derived palynomorphs indicate freshwater environments. These species of green algae, represented in the fossil record by groups such as *Tetraporina* and *Botrococcus*, are found in oxic freshwater environments. However, because of the low preservation potential, they may not be observed in areas without the right preservation conditions, thus a lack of algal palynomorphs isn't always an indicator of a dysoxic palaeoenvironment.

3.4 Palynofacies Analysis

Analysis of particulate organic matter is done by studying the relative abundance of material in each category classified in Figure 3.2 as well as looking at several key ratios. Relative abundances in each category are proxies for certain environments and/or climates. A high relative abundance of opaque phytoclasts indicates a distal depositional environment and/or

post depositional oxidation (Fig. 3.3). Conversely, a high relative abundance of translucent phytoclasts indicates proximal deposition. Equidimensional phytoclasts are indicative of a high degree of turbulent transport. A high abundance of cuticles and large phytoclasts indicate a proximal depositional environment and low energy transport. In terms of the palynomorphs and their role as a proxy for climate, it is expected that the relative abundances of monosaccate pollen grains would decrease going up the stratigraphy and the relative abundances of bisaccate grains would increase based on previous work (see section 1.4) (Falcon, 1984; Götz & Ruckwied, 2014). The relative abundances of spores give an indication of the composition of the lowland vegetation and the AOM and DOM as well as algae give clues as to the dominant environment at the time of deposition.

The ratios studied are (1) the opaque:translucent phytoclast ratio, (2) the equidimensional:blade/needle-shaped phytoclast ratio and (3) the spore:pollen ratio. The spore:pollen ratio allows one to determine the lowland and highland vegetation, as well as to identify dominant parent plants in the local environment. The phytoclast ratios can then be used to determine the type of transport occurring at the time of deposition.

Parameter	Interpretation of high (relative) values
opaque:translucent phytoclasts (other than cuticle)	Long distance or duration of transport of phytoclasts i.e. distal depositional environments removed from sources of fresh phytoclasts. Low TOC values typical in oxidizing environments, particles small and more equidimensional. Especially characteristic of basinal and distal shelf sediments deposited during high sea levels OR Postdepositional oxidation within sandy subaerial sediments, and/or soils (especially under seasonal or tidally fluctuating water table conditions). OR Local reworking from sediments of high maturation level OR Localized high flux of charcoal following wildfires and subsequently increased runoff.
equant:lath opaque phytoclast ratio	Proximity to fluvio-deltaic source area, low transport distance (especially applies where equant = largest particles; if this is not true interpretation may be opposite).
undegraded:degraded phytoclast ratio	Moderately distal oxic environments where delicate constituents have been eliminated but more resistant material is well preserved OR Distal settings in which angular refractory opaque phytoclasts have become selectively concentrated OR Areas of active redeposition, where relatively undegraded material is introduced from a proximal source area (especially at lower sea-levels where shelf widths are relatively small). The mean apparent preservation state is typically lower than in the previous case, due to co-redeposition of less resistant material.
% cuticle (of phytoclasts)	Most typical of: Fluvio-deltaic, prodelta, or estuarine-mangrove facies OR Proximal siliciclastic submarine fan facies (including sandy upper to mid-fan channel or overbank facies)
phytoclast particle size	Large particle sizes (coarse fraction) indicate: Proximity to fluvio-deltaic source(s) of terrestrial organic matter OR Active redeposition from a fluvio-deltaic source area, as in turbidites (especially basal parts) AND/OR Sandy or silty sediments (due to hydrodynamic equivalence).

Figure 3.3: Phytoclast palynofacies parameters used for palaeoenvironment interpretation and reconstruction (from Tyson, 1995).

4. Results

4.1 Description of Samples

4.1.1 Palesa

The Palesa locality represents the northern-most sample set taken in the Witbank Coalfield. No intraseam parting was present at this locality. Instead, siltstones of varying thicknesses were intercalated with the coals. The total thickness of the coal seam was 8 m and 10 samples were taken from this locality. Between 501 and 509 particles were counted for each of the samples taken. Samples are numbered 1 to 10 from the bottom to the top.

The relative abundance of palynomorphs (Fig. 4.1) shows a number of prominent trends. The monosaccate pollen grains decrease in abundance replaced by a dominant bisaccate pollen assemblage as one moves up the stratigraphy. At 4 m, even the taeniate bisaccates have a higher abundance than the monosaccate pollen grains, although they never become more abundant than the non-taeniate bisaccate pollen grains. Monolete spores are seen in the first 3 m of the section and the trilete spore abundance decreases dramatically above this interval. High trilete spore abundance appears to correlate with high abundance of AOM while higher abundances of DOM and algae can be associated with lower abundances of trilete spores and AOM.

The high abundances of trilete spores and AOM also correlate with high abundances of opaque phytoclasts (Fig. 4.2). At 4 m and again at 6-8 m, there is a decrease in both the spore:pollen ratios as well as the opaque:translucent ratios. Across the whole coal seam, equidimensional phytoclasts are dominant especially at 6-8 m. The equidimensional:blade-shaped ratio is relatively similar in samples 1 to 7 (3.33, 3.44, 3.9, 4.07, 4.5, 5.5, 4.2) and slightly higher in samples 9 and 10 (7.36, 6.78), but shows a large increase in sample 8 (12.54) (Fig. 4.3).

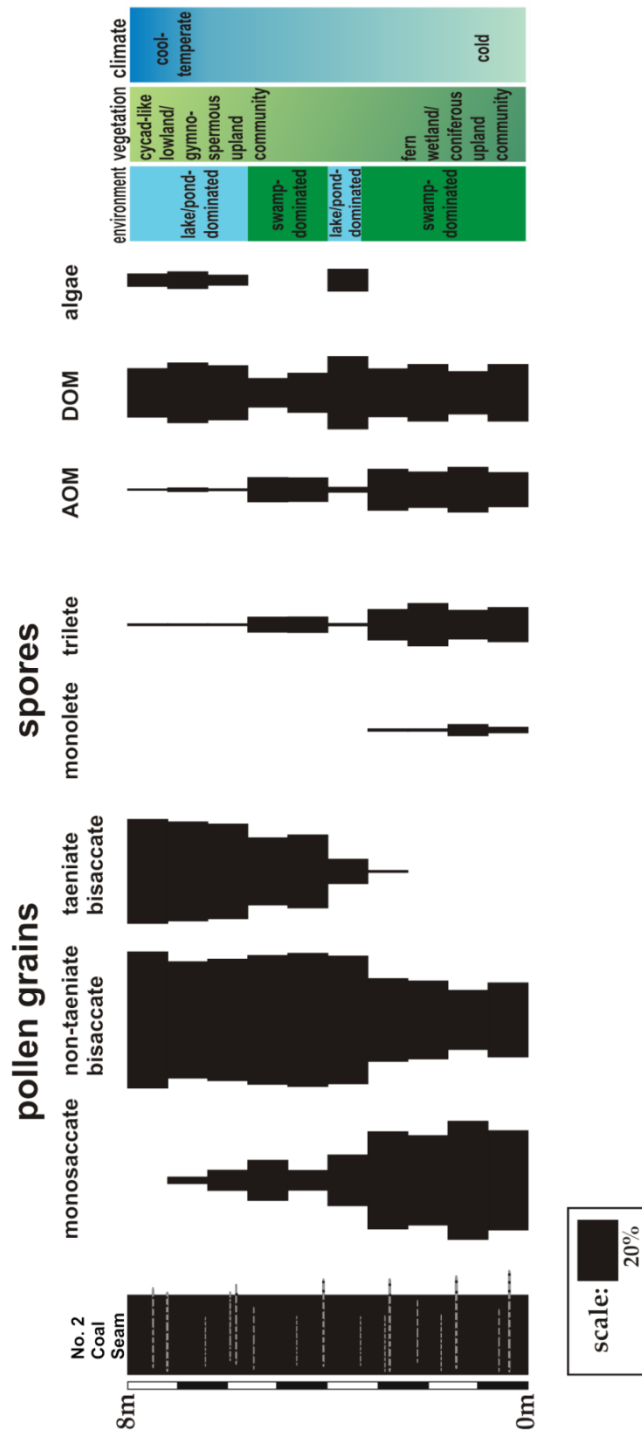


Figure 4.1: Spindle diagram showing relative abundance of sporomorphs, AOM, DOM and freshwater algae at Palesa locality. AOM – amorphous organic matter, DOM – degraded organic matter.

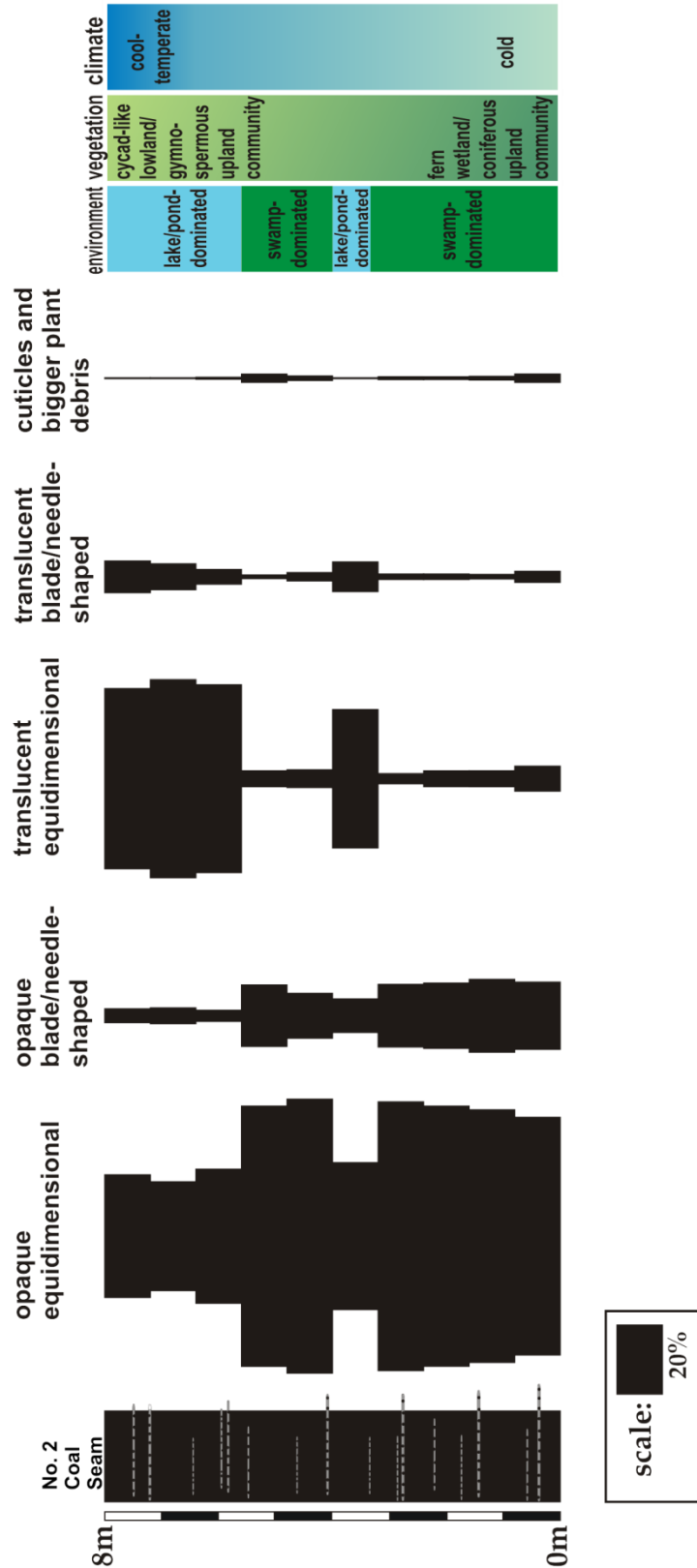


Figure 4.2: Spindle diagram showing relative abundances of phytoclasts at Palesa locality.

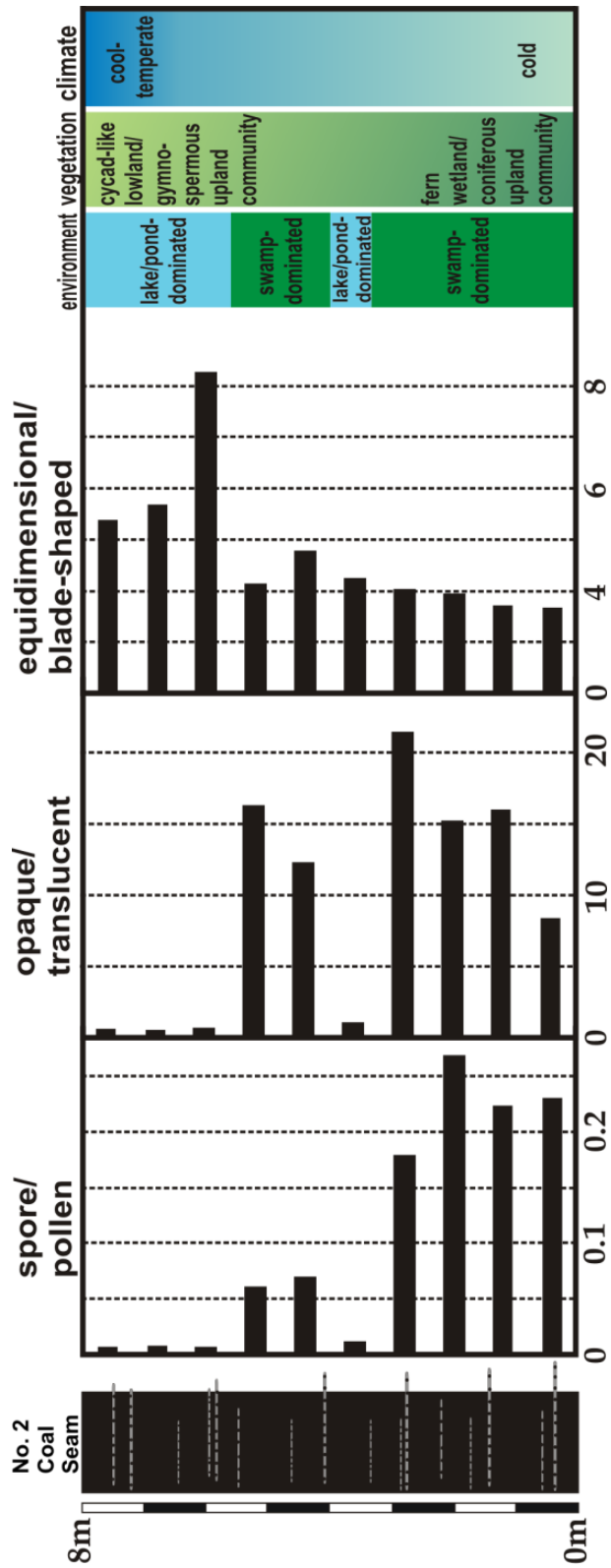


Figure 4.3: Graph showing spore:pollen, opaque:translucent phytoclast and equidimensional:blade-shaped phytoclast ratios at Palesa locality.

4.1.2 HWH1418

The HWH1418 locality represents the central eastern part of the Witbank Coalfield. A 1 m thick sandstone intraseam parting is present at this locality. 14 samples were taken covering a total seam thickness of 6 m. The Lower Coal Seam is 1.5 m thick and the Upper Coal Seam is 3.5 m thick. Between 501 and 508 particles were counted for each of the samples taken. Samples are numbered 1 to 14 from the bottom to the top.

Lower Coal Seam

The monosaccate pollen grains are most abundant in the Lower Coal Seam but the non-taeniate bisaccate pollen grains have a similar abundance (Fig. 4.4). No taeniate bisaccate pollen grains are present in the Lower Coal Seam. This seam has the highest abundances of spores and AOM and low abundances of DOM. No algae was observed. In terms of phytoclasts, this seam has high abundances of opaque equidimensional material and slightly higher abundances of cuticles and larger plant debris than the Upper Coal Seam (Fig. 4.5). This seam has very high spore:pollen ratios (2.4, 2.18, 2.29, 3.18) (Fig. 4.6).

Intraseam Parting

In the intraseam parting, the monosaccate pollen grains start to decrease in abundance while the bisaccate pollen grains increase (Fig. 4.4). Taeniate bisaccate pollen grains appear in small abundances for the first time. The spores decrease and AOM was not observed. DOM has the highest relative abundance in the intraseam parting and algae does appear in small abundances. The parting has the highest ratio of opaque:translucent (11.59, 12.9, 8.5) and equidimensional:blade/needle-shaped phytoclasts (10.19, 11.26, 14.64) (Fig. 4.6).

Upper Coal Seam

The monosaccate pollen grains decrease in this seam and eventually disappear (Fig. 4.4). The bisaccate pollen grains are most abundant in this seam and the taeniates have a high abundance. The spores decrease to low abundances and monolet spores are not observed in

some of the samples. AOM is present in low abundances. DOM and algae is present in moderate abundances. Opaque equidimensional phytoclasts have their lowest abundances in this seam, while the translucent equidimensional phytoclasts have their highest abundances in this seam (Fig. 4.5). The spore:pollen (0 to 0.07), opaque:translucent (0.62 to 1.17) and equidimensional:blade-shaped ratios are all relatively low (2.45 to 5.55) (Fig. 4.6).

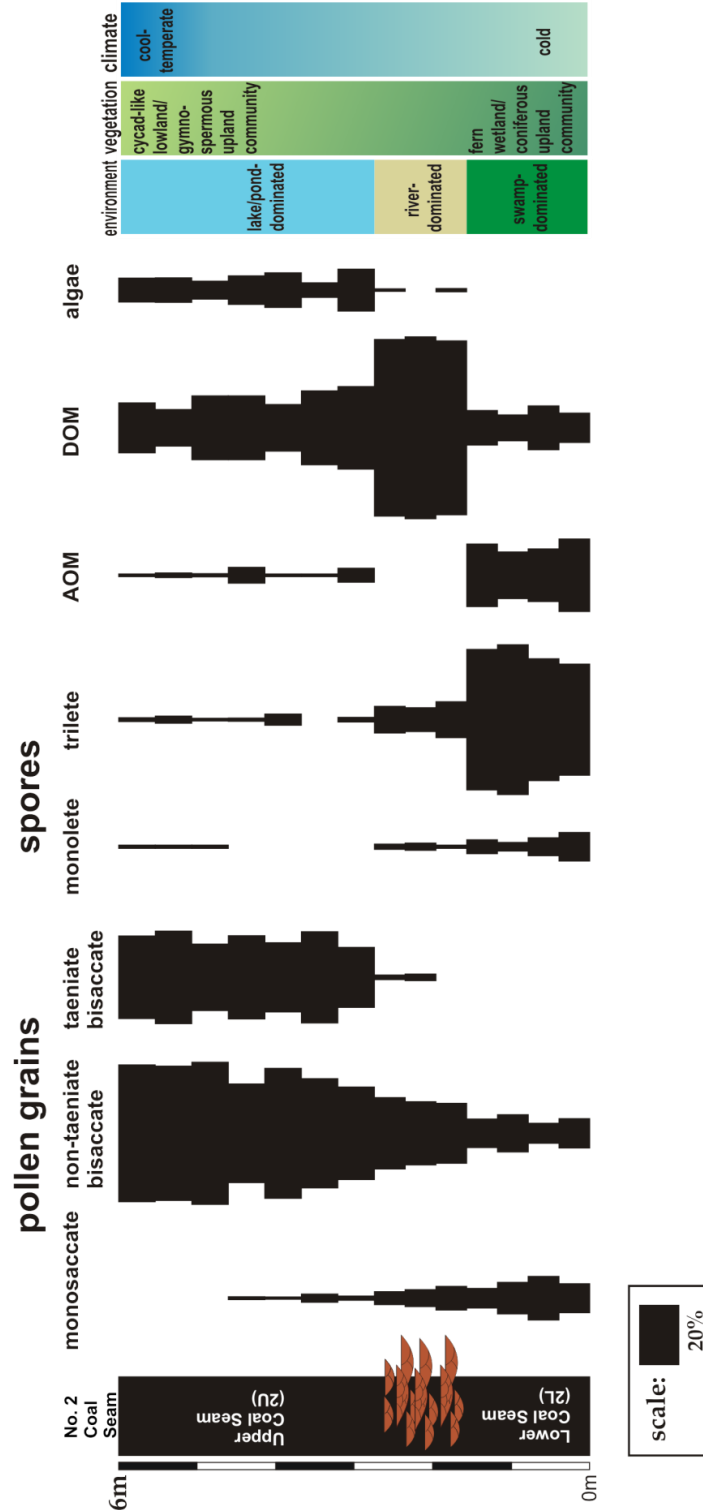


Figure 4.4: Spindle diagram showing relative abundances of sporomorphs, AOM, DOM and freshwater algae at HWH1418 locality. AOM – amorphous organic matter, DOM – degraded organic matter.

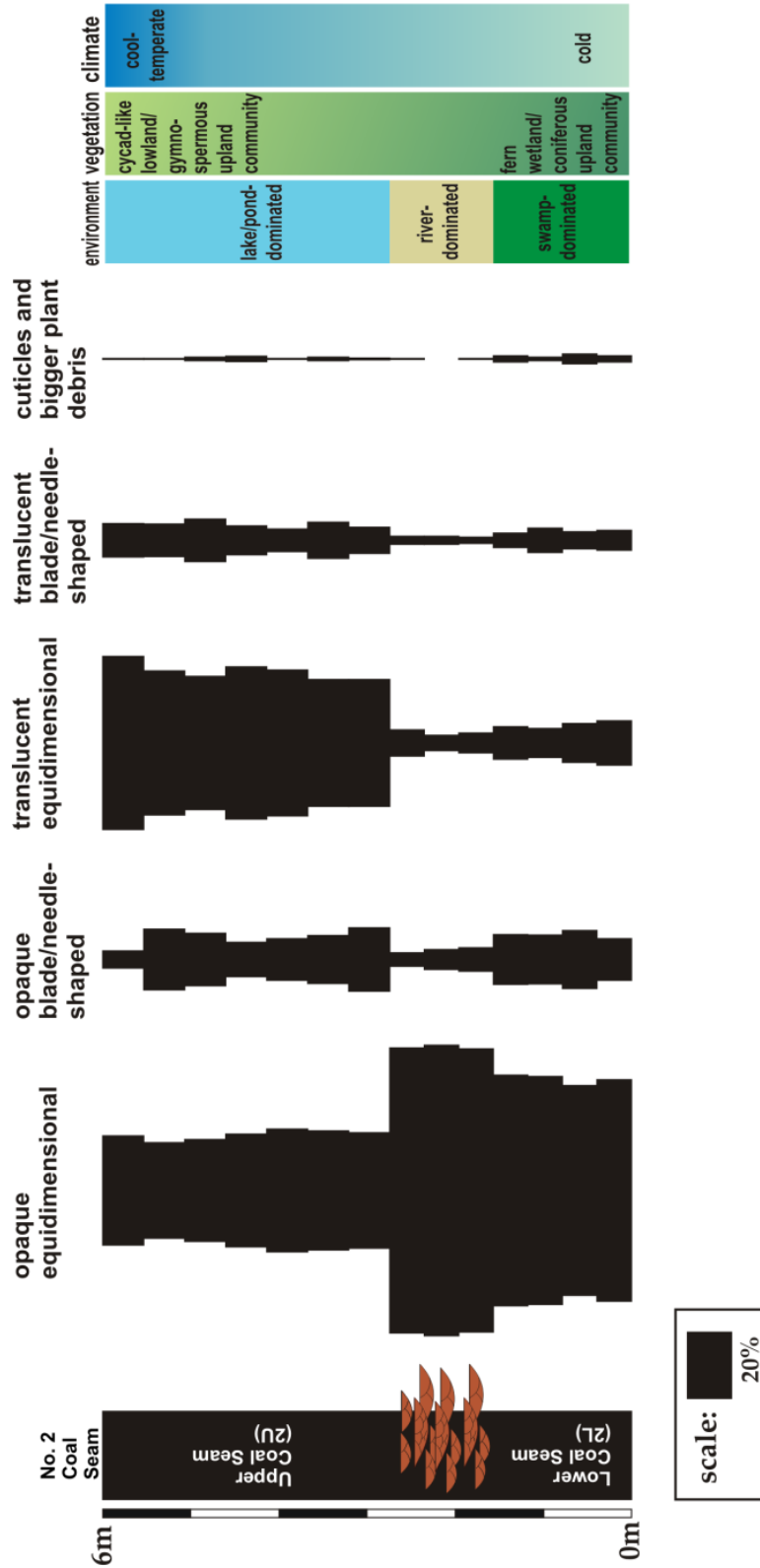


Figure 4.5: Spindle diagram showing relative abundances of phytoclasts at HWH1418 locality.

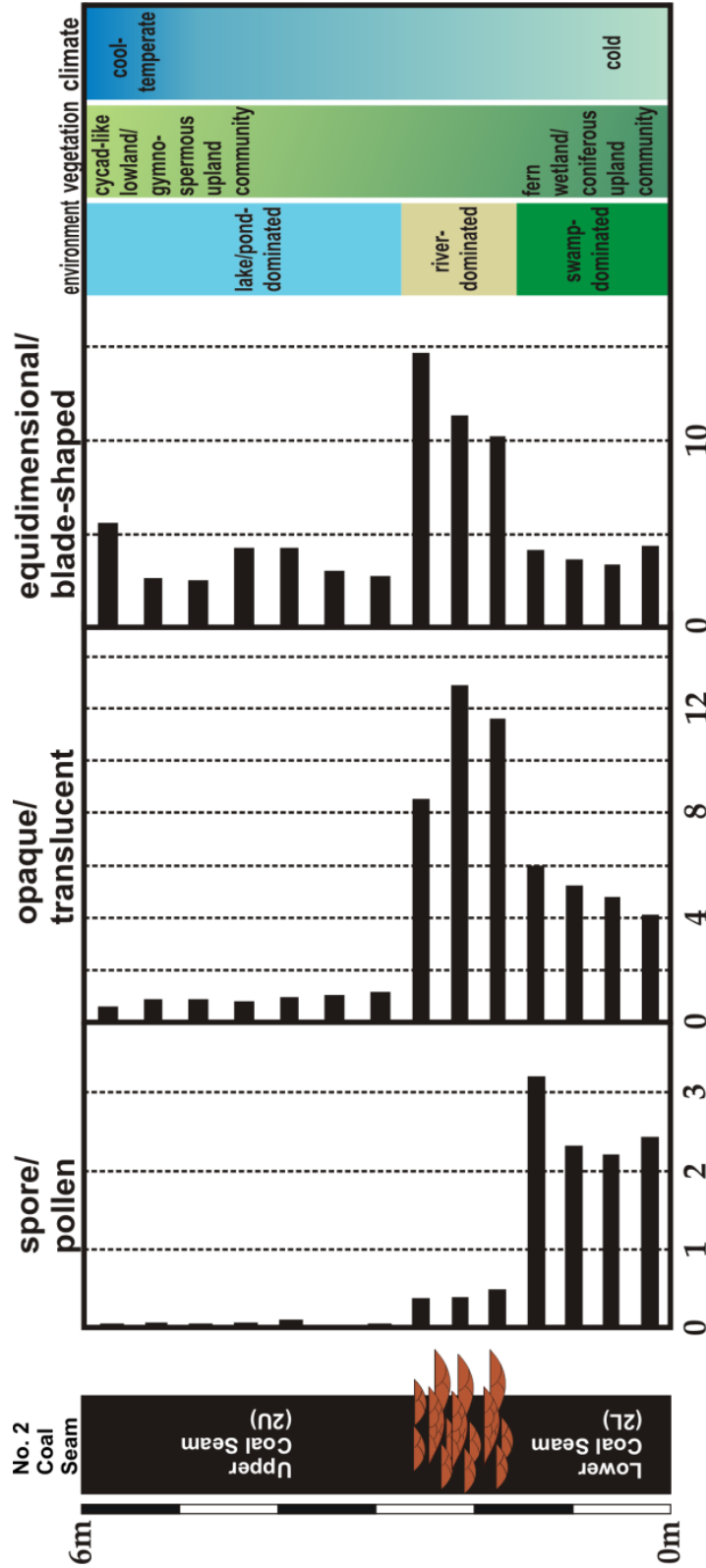


Figure 4.6: Graph showing spore:pollen, opaque:translucent phytoclast and equidimensional:blade-shaped phytoclast ratios at HWH1418 locality.

4.1.3 BHS14

The BHS14 locality represents the central western sample set taken in the Witbank Coalfield. No intraseam parting was present at this locality. Sampling was done in siltstones of varying thicknesses, which were intercalated with the coals. The total thickness of the coal seam was 3.6 m and 10 samples were taken from this locality. Between 501 and 511 particles were counted for each of the samples taken. Samples are numbered 1 to 10 from the bottom to the top.

Again one sees the trend of decreasing abundances of monosaccate pollen grains and increasing abundances of bisaccate pollen grains (Fig. 4.7). Taeniate bisaccate pollen grains appear in the upper 1.6 m. Spores are present in the highest abundances in the first two meters. Monolete spores decrease and disappear above this, while trilete spores decrease to relatively low abundances. The AOM and DOM have relatively unchanging abundances throughout the sequence except in sample 7 taken at 2.5 m. At this interval the AOM is relatively low while the DOM shows a high increase in abundance. This is also the only sample where algae is observed.

In terms of phytoclasts, the abundances of the opaque equidimensional and the translucent blade-shaped phytoclasts seem to change very little but the opaque blade-shaped show an increase while the translucent equidimensional particles show a decrease (Fig. 4.8). All the phytoclast categories show large changes in sample 7 and this is also reflected in the ratios. The spore:pollen ratio decreases to less than 0.08 in sample 7 and remains under 0.2 in the upper three samples (Fig. 4.9).

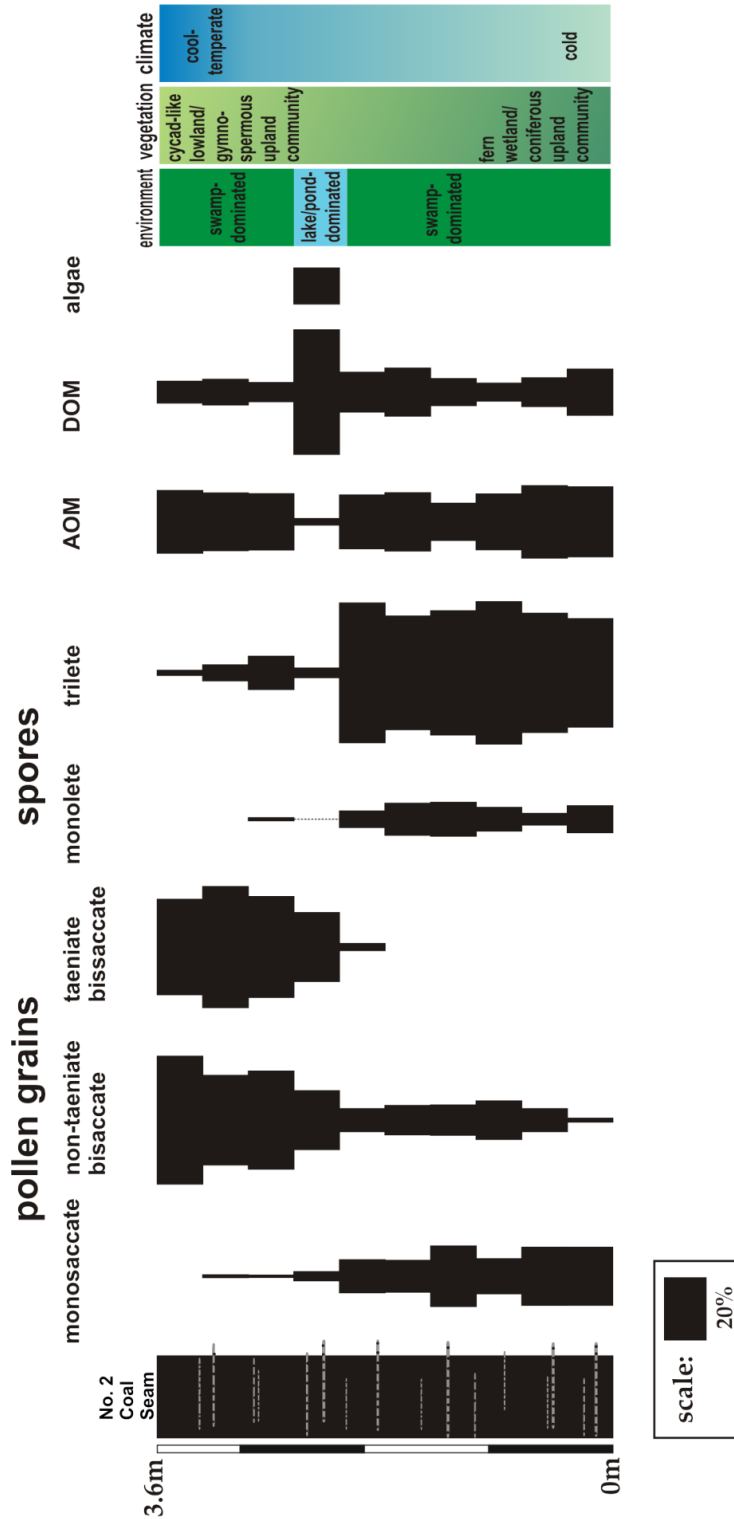


Figure 4.7: Spindle diagram showing relative abundances of sporomorphs, AOM, DOM and freshwater algae at BHS14 locality. AOM – amorphous organic matter, DOM – degraded organic matter.

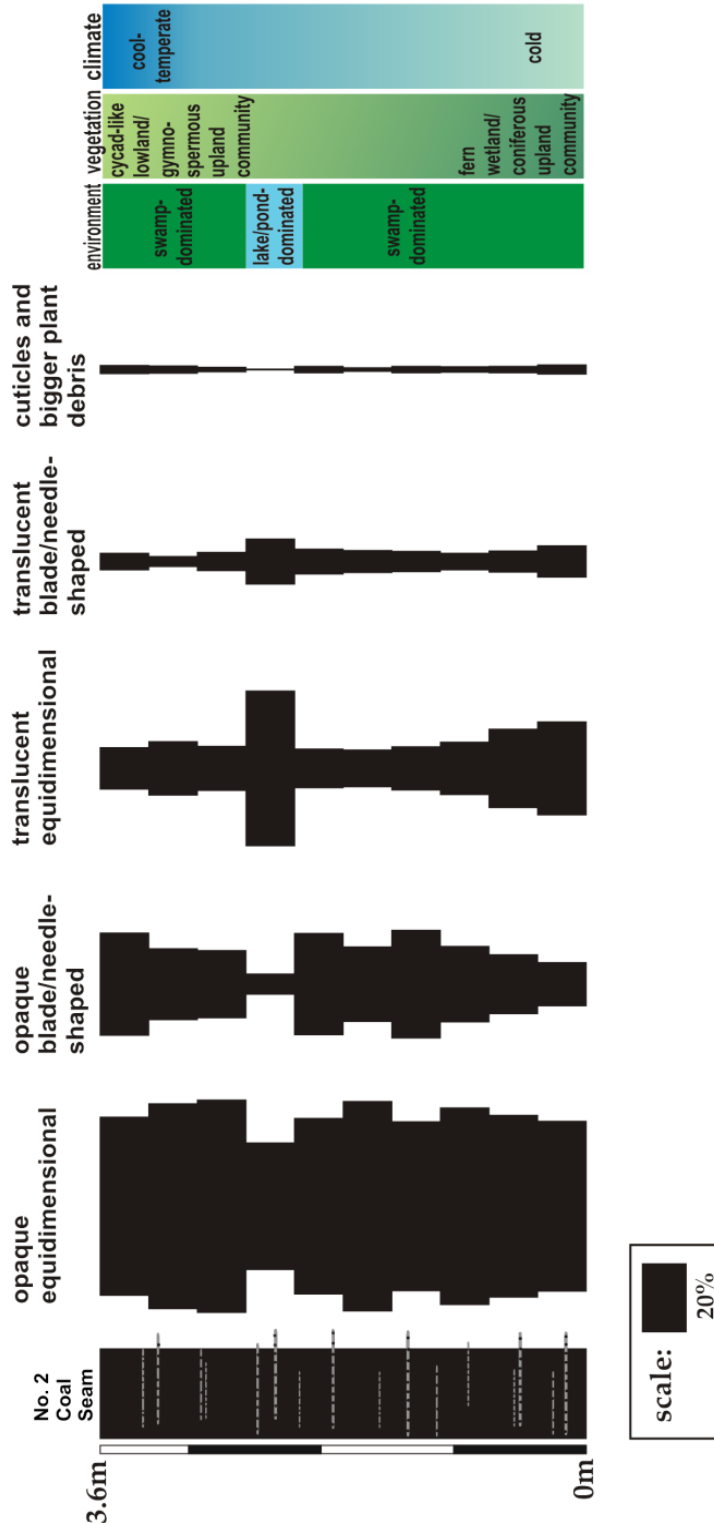


Figure 4.8: Spindle diagram showing relative abundance of phytoclasts at BHS14 locality.

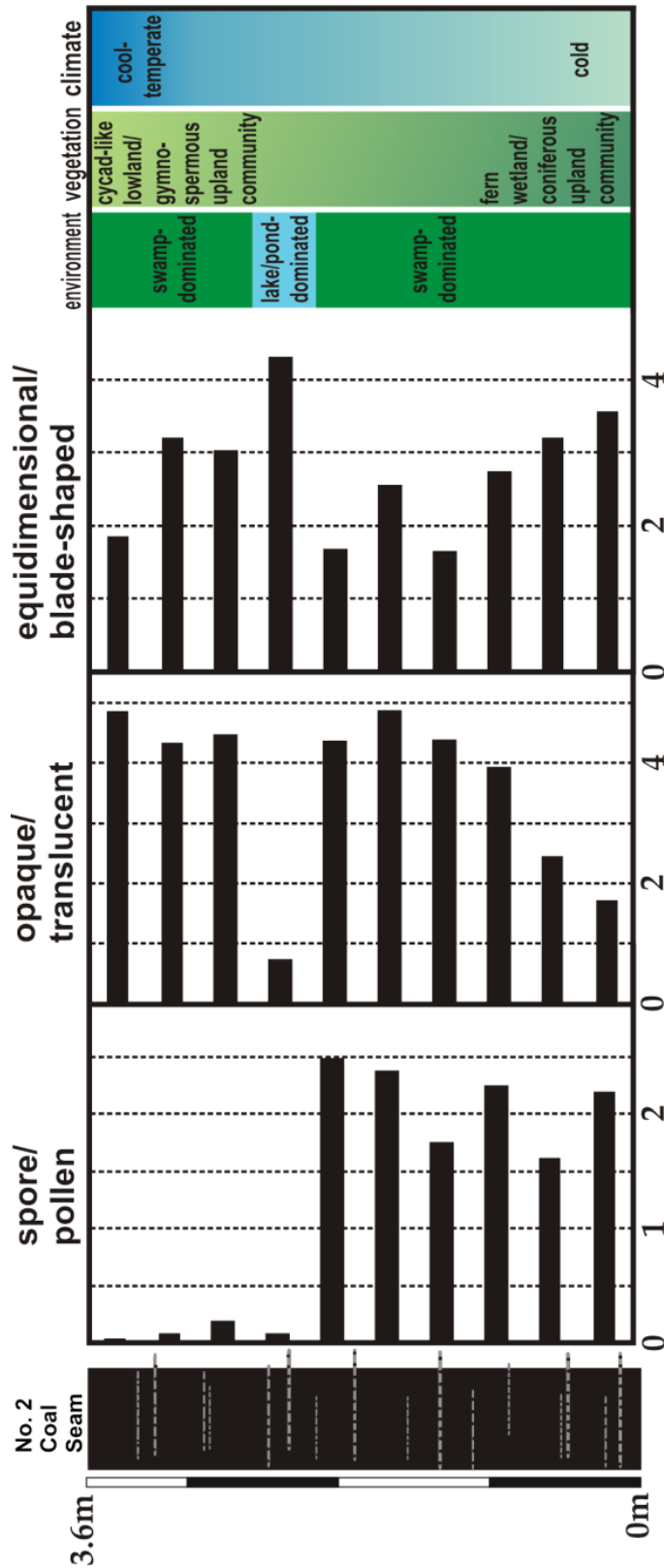


Figure 4.9: Graph showing spore:pollen, opaque:translucent phytoclast and equidimensional:blade-shaped phytoclast ratios at BHS14 locality.

4.1.4 ALBN11

The ALBN11 locality represents the southern part of the Witbank Coalfield close to the Smithfield Ridge. A 0.4 m thick sandstone intraseam parting is present at this locality. 8 samples were taken covering a total seam thickness of 6 m. The Lower Coal Seam is 2 m thick and the Upper Coal Seam is 3.6 m thick. Between 501 and 591 particles were counted for each of the samples taken. Samples are numbered 1 to 8 from the bottom to the top.

Lower Coal Seam

As with the other sample sets, the monosaccate pollen grains have the highest abundance in the Lower Coal Seam and non-taeniate bisaccates are also present (Fig. 4.10). No taeniate bisaccate pollen grains were observed in the Lower Coal Seam. Monolete and trilete spores are both present in the Lower Coal Seam, however no monoletes were observed in the second sample while triletes show the highest relative abundance. DOM is present in relatively moderate abundances in the Lower Coal Seam. No AOM or algae was observed. The equidimensional:blade-shaped ratio is relatively high (Fig. 4.12). The first two samples have opaque:translucent ratios quite close to 1 but the third sample has a ratio of 0.54.

Intraseam Parting

The sandstone parting features monosaccate, non-taeniate bisaccate and taeniate bisaccate pollen grains. Spore abundances remain relatively low. AOM appears in small abundance and DOM shows a huge increase in the parting. No algae was observed (Fig. 4.10). There are no big differences in the phytoclast ratios compared to the Lower Coal Seam but the relative abundance of the cuticles and larger plant debris is higher than in the Upper and Lower Coal Seam (Fig. 4.11).

Upper Coal Seam

In the Upper Coal Seam, the monosaccate pollen grains decrease and disappear while the bisaccate pollen grains increase (Fig. 4.10). Taeniate bisaccate pollen grains are only present in

the upper two samples. Monolete spores remain relatively low but the trilete spores increase in abundance in samples 6 and 7. AOM is present with low abundances in samples 5 and 6 and increases slightly in sample 7 but is not observed in sample 8. DOM occurs in moderate abundances in the Upper Coal Seam. Algae are observed in samples 5, 6, and 8. The opaque:translucent ratio is very high in sample 7 (1.2) but the equidimensional:blade-shaped ratios show little variance in the Upper Coal Seam (3.32 to 3.82) (Fig. 4.12).

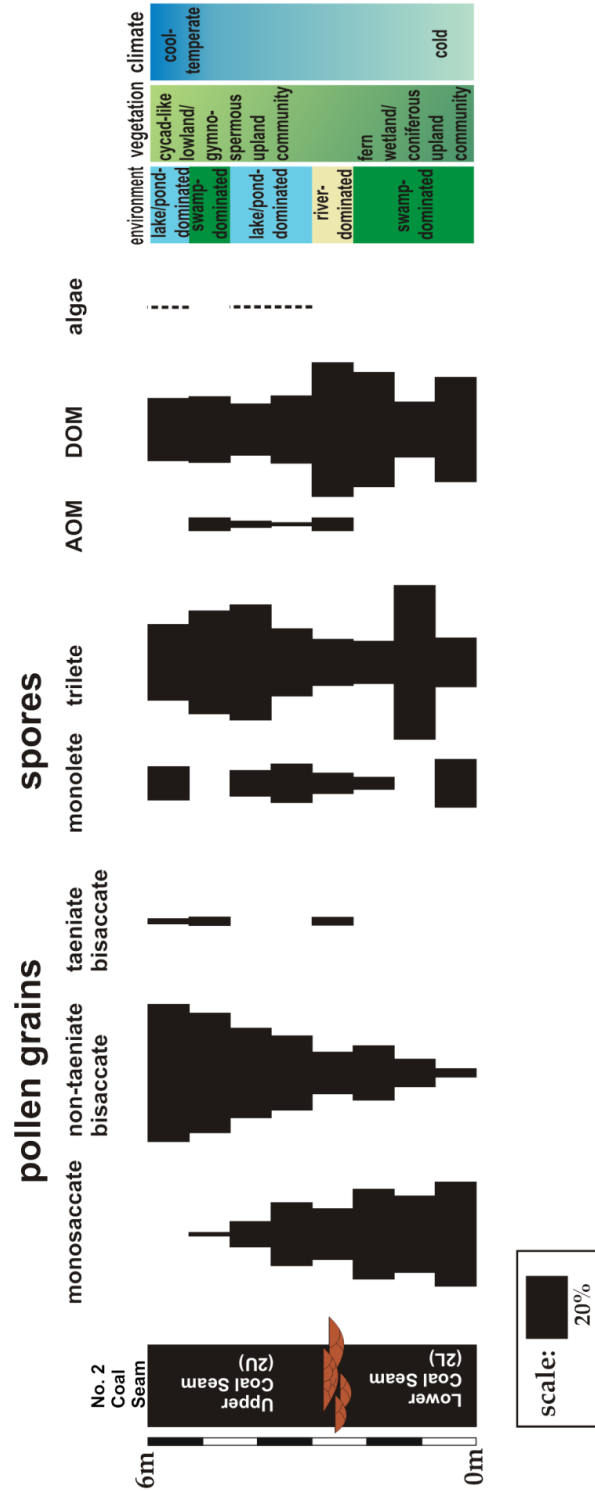


Figure 4.10: Spindle diagram showing relative abundances of sporomorphs, AOM, DOM and freshwater algae at ALBN11 locality. AOM – amorphous organic matter, DOM – degraded organic matter.

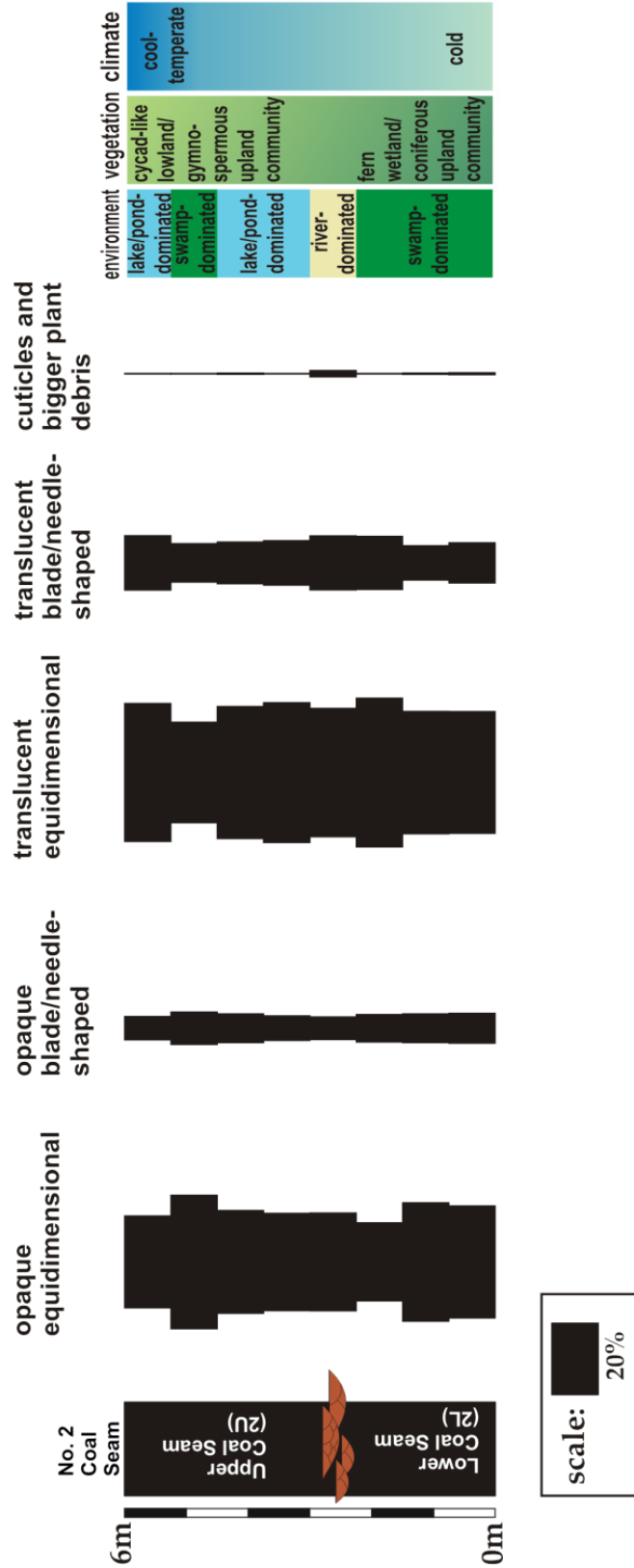


Figure 4.11: Spindle diagram showing relative abundances of phytoclasts at ALBN11 locality.

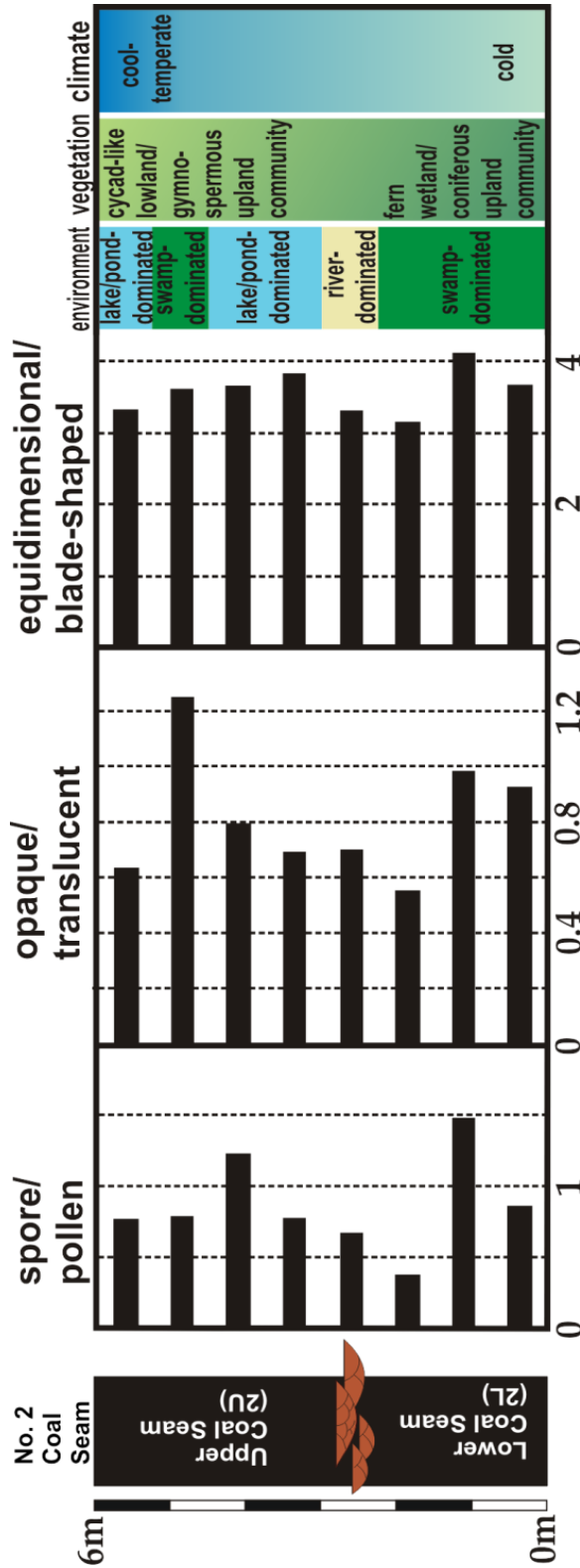


Figure 4.12: Graph showing spore:pollen, opaque:translucent phytoclast and equidimensional:blade-shaped phytoclast ratios at ALBN11 locality.

4.1.5 K114314

The K114314 locality represents the northern part of the Highveld Coalfield close to the Smithfield Ridge. A 0.3 m thick sandstone intraseam parting is present at this locality. 12 samples were taken covering a total seam thickness of 5.2 m. The Lower Coal Seam is 1.8 m thick and the Upper Coal Seam is 2.1 m thick. Between 501 and 514 particles were counted for each of the samples taken. Samples are numbered 1 to 12 from the bottom to the top.

Lower Coal Seam

Monosaccate pollen grains are present in moderate abundances and bisaccates are present in low abundances but show an increase (Fig. 4.13). No taeniate bisaccate pollen grains are present in the Lower Coal Seam. Spores are present in high abundances with triletes being dominant. AOM and DOM are present in similar abundances. No algae was observed in the Lower Coal Seam. The equidimensional:blade-shaped phytoclast ratio is relatively low (4.18 to 8.93) while the opaque:translucent ratio is relatively high and increases (from 1.52 to 2.39) (Fig. 4.15). The spore:pollen ratio is high but decreases (from 2.06 to 1).

Intraseam Parting

The pollen grain abundances in the intraseam parting are similar to the Lower Coal Seam but taeniate bisaccate pollen grains are also present in low abundances. Spores and AOM decrease to very low abundances while DOM increases to a high abundance (Fig. 4.13). Algae is present in low abundances. The equidimensional:blade-shaped (30.5, 20.33) and opaque:translucent (2.57, 2.76) phytoclast ratios are both high while the spore:pollen ratio is low (0.26, 0.25) (Fig. 4.15).

Upper Coal Seam

Monosaccate pollen grains decrease in relative abundance and disappear in the Upper Coal Seam while the bisaccates increase towards the top of the sequence (Fig. 4.15). Samples 8, 11 and 12 show similar signatures of little to no spores, very low AOM, moderate DOM and low to

moderate algae. Samples 9 and 10 have slightly higher abundances of trilete spores and AOM and lower abundances of DOM and algae compared to samples 8, 11 and 12. The phytoclast abundances show similar trends with lower opaque equidimensional abundances in samples 8, 11 and 12 and higher abundances in samples 9 and 10 (Fig. 4.14). Conversely the translucent equidimensional phytoclasts have a higher abundance in samples 8, 11 and 12, and lower abundances in samples 9 and 10. The opaque:translucent ratio is low in samples 8 (0.94), 11 (0.94) and 12 (0.72) but high in samples 9 (3.03) and 10 (2.93). The equidimensional:blade-shaped ratio is low throughout the Upper Coal Seam but does show a slight increase in samples 9 (7.15) and 10 (8.2) (Fig. 4.15).

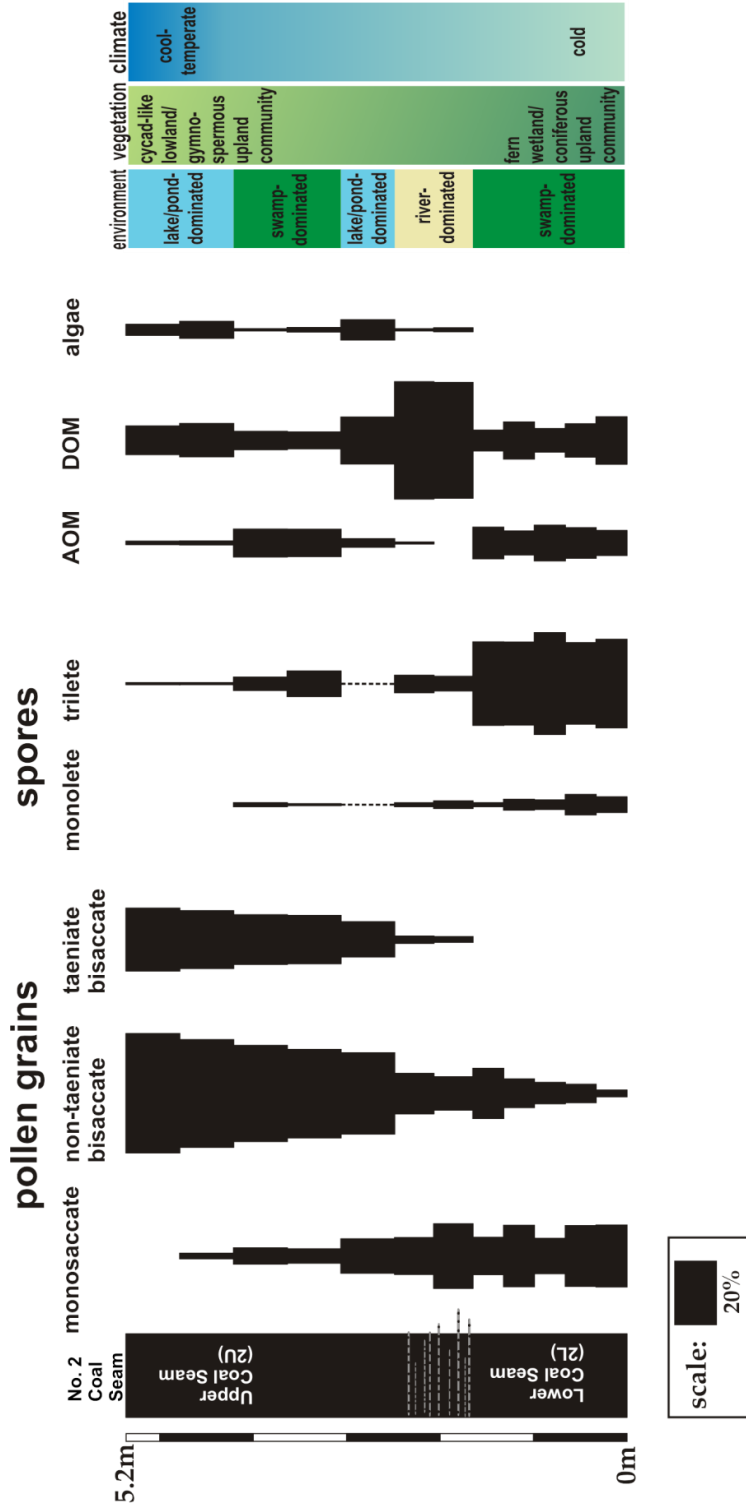


Figure 4.13: Spindle diagram showing relative abundances of sporomorphs, AOM, DOM and freshwater algae at K114134 locality. AOM – amorphous organic matter, DOM – degraded organic matter.

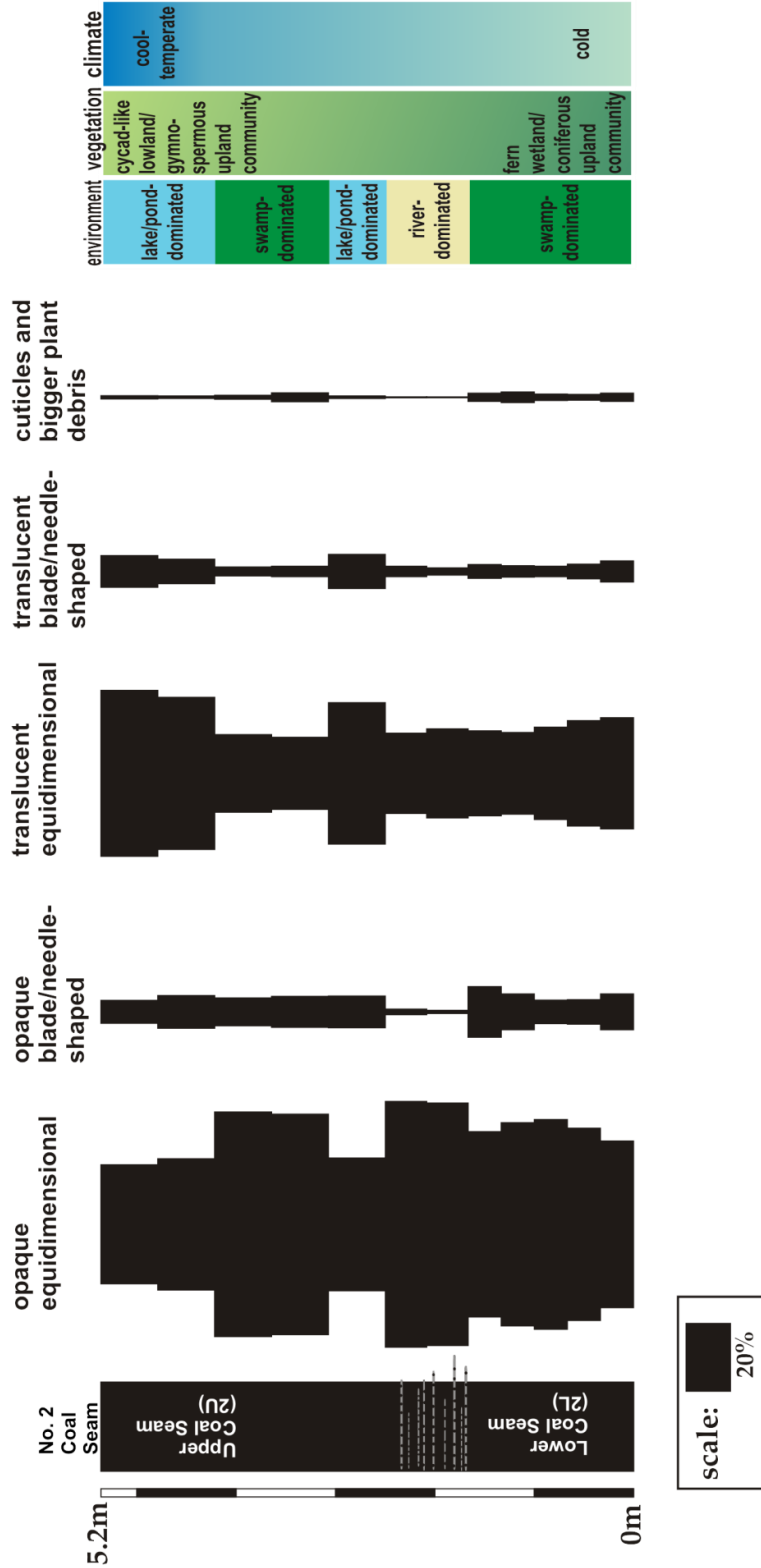


Figure 4.14: Spindle diagram showing relative abundances of phytoclasts at K114134 locality

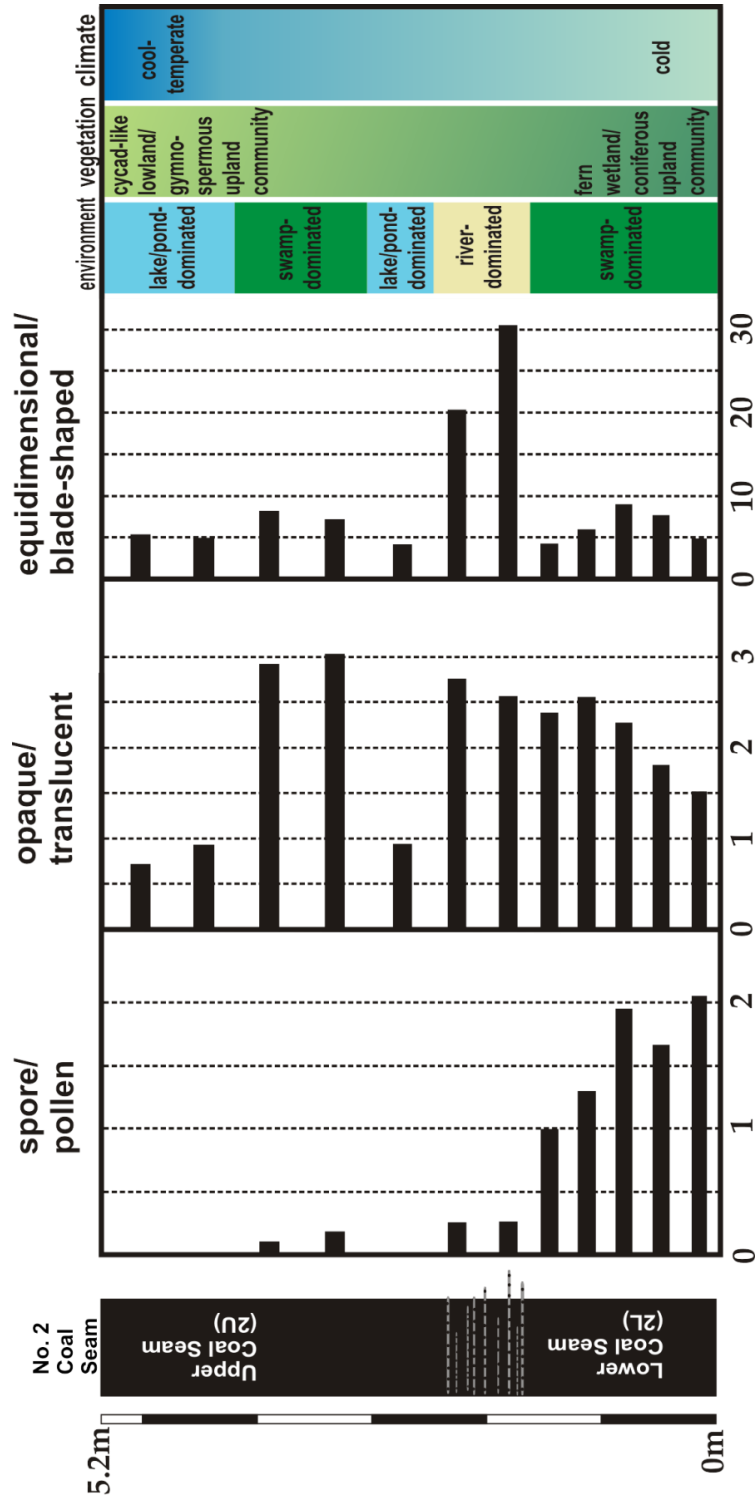


Figure 4.15: Graph showing spore:pollen, opaque:translucent phytoclast and equidimensional:blade-shaped phytoclast ratios at K114314 locality.

4.1.6 S542145

The S542145 locality is located in the central-western part of the Highveld Coalfield and represents the southernmost locality studied. A 0.3 m thick siltstone intraseam parting is present at this locality. 8 samples were taken covering a total seam thickness of 5 m. The Lower Coal Seam is 2 m thick and the Upper Coal Seam is 2.3 m thick. Between 501 and 509 particles were counted for each of the samples taken. Samples are numbered 1 to 8 from the bottom to the top.

Lower Coal Seam

The monosaccate pollen abundance is moderately high in sample 1 but decreases to low abundance in samples 2 and 3 (Fig. 4.16). Bisaccate non-taeniate pollen grains are present in the Lower Coal Seam increasing to moderate to high abundances in sample 2 and 3. Bisaccate taeniate pollen grains are not present in the Lower Coal Seam. Spore:pollen ratio is high (1.22, 1.47, 1.72) in this seam (Fig. 4.18) but the monolete spores have a higher abundance than the trilete spores (Fig. 4.16). AOM and freshwater algae are only present in sample 3 and the DOM shows a moderate abundance. The opaque:translucent and the equidimensional:blade-shaped ratios both decrease from 3.46 to 1.04 and from 1.96 to 1.01 respectively in this seam. The abundance of opaque equidimensional phytoclasts is particularly low in sample 3 and the relative abundances both equidimensional and blade-shaped translucent phytoclasts show an increase (Fig. 4.17).

Intraseam Parting

The monosaccate pollen abundance is very low in the siltstone parting (Fig. 4.16). No bisaccate taeniate pollen grains were observed. The spore:pollen ratio also shows a decrease in this sample (0.89) while the opaque:translucent ratio shows a significant increase (9.85) (Fig. 4.18). The abundance of opaque equidimensional phytoclasts is particularly high in this sample. No AOM or freshwater algae were observed but the abundance of DOM is very high. Larger plant debris and cuticles were not observed in this sample (Fig. 4.17).

Upper Coal Seam

The monosaccate pollen grain abundances are lowest in the Upper Coal Seam, but are still present in all samples (Fig. 4.16). The abundance of non-taeniate bisaccate pollen grains is lowest in sample 5 but increases to high abundance in samples 6, 7 and 8. Taeniate bisaccate pollen grains also appear in sample 5 and increase in abundance to the top of the sequence. The spore:pollen ratio is very high in sample 5 (1.83) but drops sharply in sample 6 (0.67) and continues to decrease in samples 7 (0.52) and 8 (0.37) (Fig. 4.18). The abundance of monolete spores remains higher than the trilete spores throughout the Upper Coal Seam. There are no significant changes in the phytoclast abundances in the Upper Coal Seam except for an increase in the equidimensional:blade-shaped phytoclast ratio in sample 6 (1.91). AOM was only observed in sample 7 in very small abundances and no freshwater algae was observed. The DOM decreases to its lowest abundances in samples 6 and 7. Larger plant debris was observed throughout the Upper Coal Seam but the abundance decreases slightly in sample 6 (Fig. 4.17).

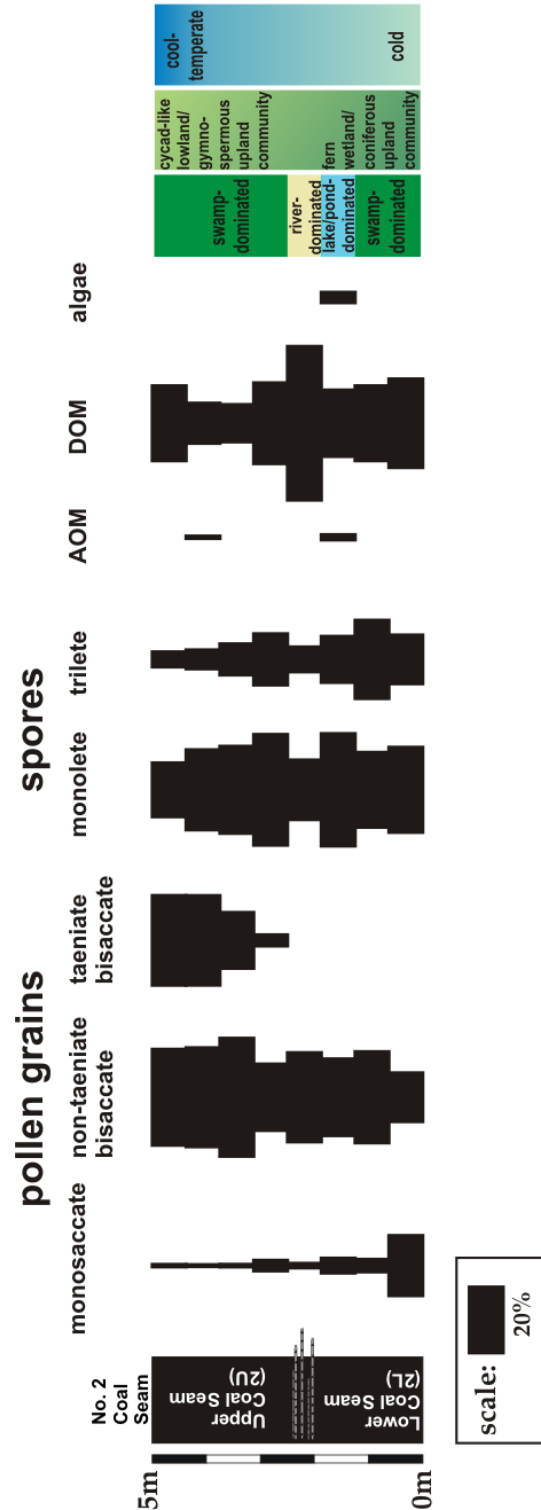


Figure 4.16: Spindle diagram showing relative abundances of sporomorphs, AOM, DOM and freshwater algae at S542145 locality. AOM – amorphous organic matter, DOM – degraded organic matter.

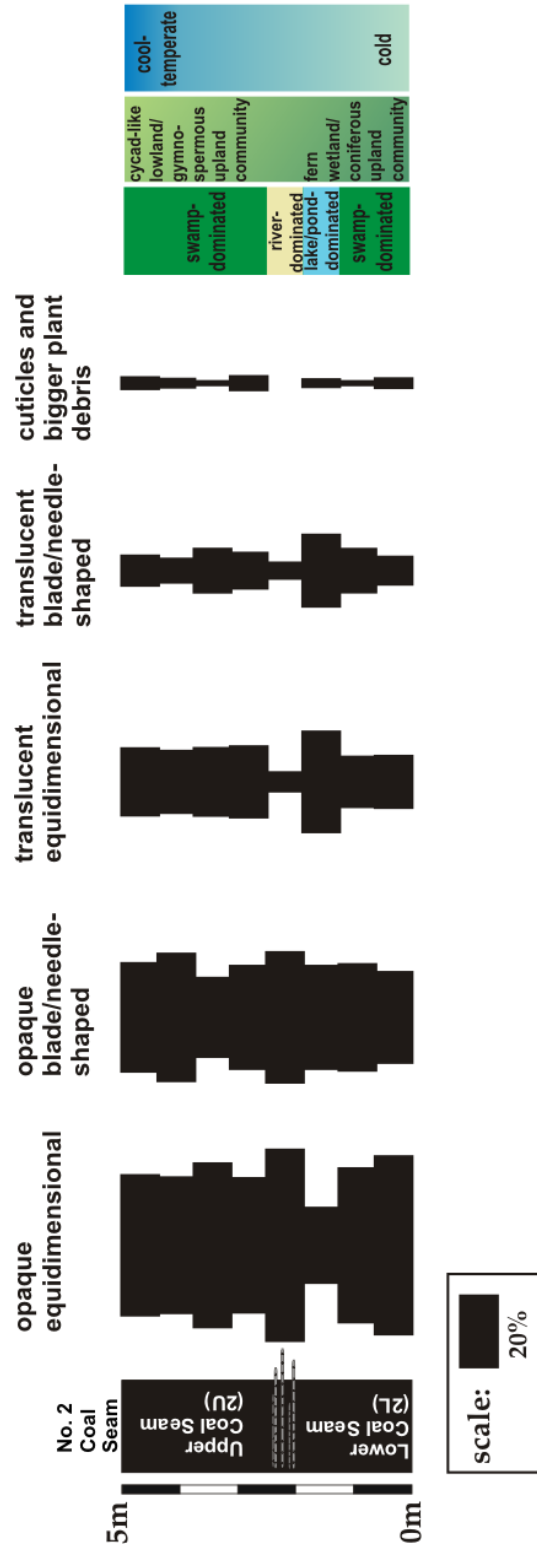


Figure 4.17: Spindle diagram showing relative abundances of phytoclasts at S542145 locality.

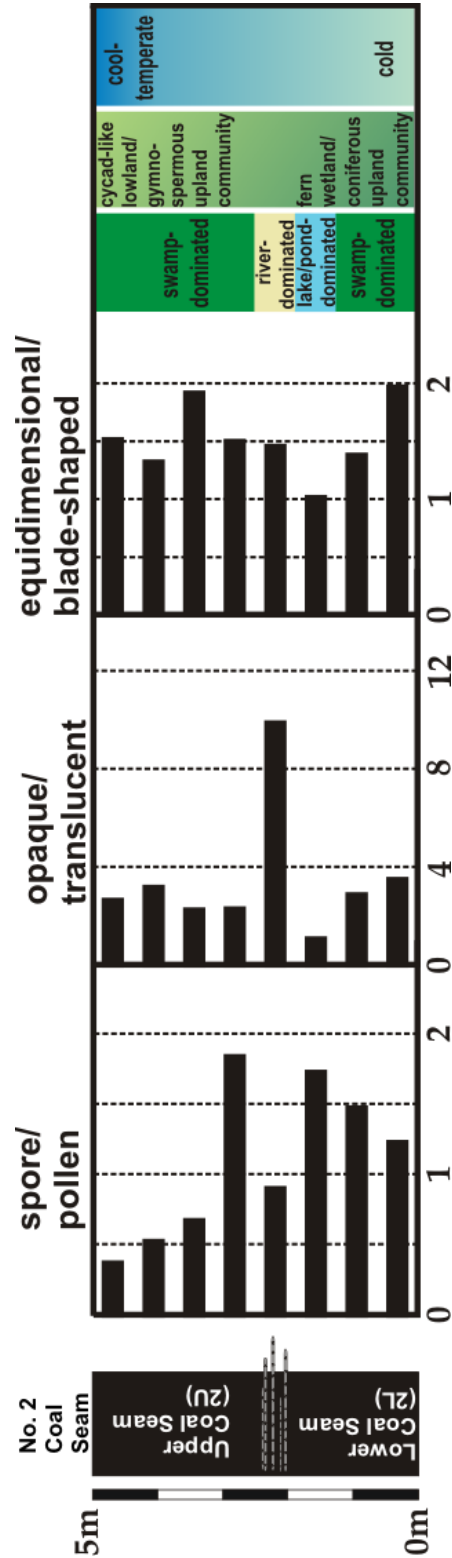


Figure 4.18: Graph showing spore:pollen, opaque:translucent phytoclast and equidimensional:blade-shaped phytoclast ratios at S542145 locality.

5. Discussion

5.1 Palaeoenvironment Analysis

The palaeoenvironment of the Lower Coal Seam is generally swamp-dominated at all localities except S542145. In the Upper Coal Seam, the palaeoenvironment varies at each locality, shifting between phases of swamp-dominated and lake-dominated environments (Plate 1, 2). Given that the palaeoenvironment is controlled by factors such as climate, topography and sedimentary input, two possible causes for the fluctuations are either due to the climate shift or to tectonic activity. The Kaapvaal Craton, which forms the basement of the Witbank and Highveld coalfields, is relatively stable at that point in the early Permian (Johnson et al., 1997). A shift in the climate from a cold to a cool-temperate climate would cause glacial retreat and increase an influx of fresh meltwater into the basin as well as altering regional precipitation patterns. Only at locality BHS14 do we see a lake-dominated environment throughout the Upper Coal Seam and only at locality S542145 do we see a swamp-dominated environment throughout. It is possible that the sampling density did not capture changes in the local palaeoenvironment but then these shifts would be minor fluctuations and may not cause noteworthy changes in the vegetation. A true interpretation of the environment can't be done without looking at multiple parameters. High opaque:translucent ratios, when coupled with high equidimensional:blade-shaped ratios, indicate a large transport distance (see figure 3.3). However, when coupled with low equidimensional:blade-shaped ratios, a high abundance of opaque phytoclasts is likely the result of post-depositional oxidation in sub-aerial sediments.

The importance of topographic controls on the palaeoenvironment should also be noted (Fig. 6.2). The palaeotopography is likely the factor which controlled distribution and thickness of the intraseam parting as well as other smaller internal partings during flooding events. The distribution of *Florinites*-type pollen associated with cordaitalean trees is limited to localities associated with palaeovalleys opening to broad swamplands (HWH1418, BHS14 and S542145). These trees likely exploit the wetter conditions in the lowlands and are able to flourish on an uneven valley floor produced by postglacial moraine deposition (Falcon, 1989) but are unable

to spread further across the broad swampland due to the established stable swamp vegetation and large meandering rivers and lakes. More studies would need to be done to determine the full extent of the distribution of these trees in relation to the valley axes, valley flanks and the drier upland areas where coniferous vegetation is dominant.

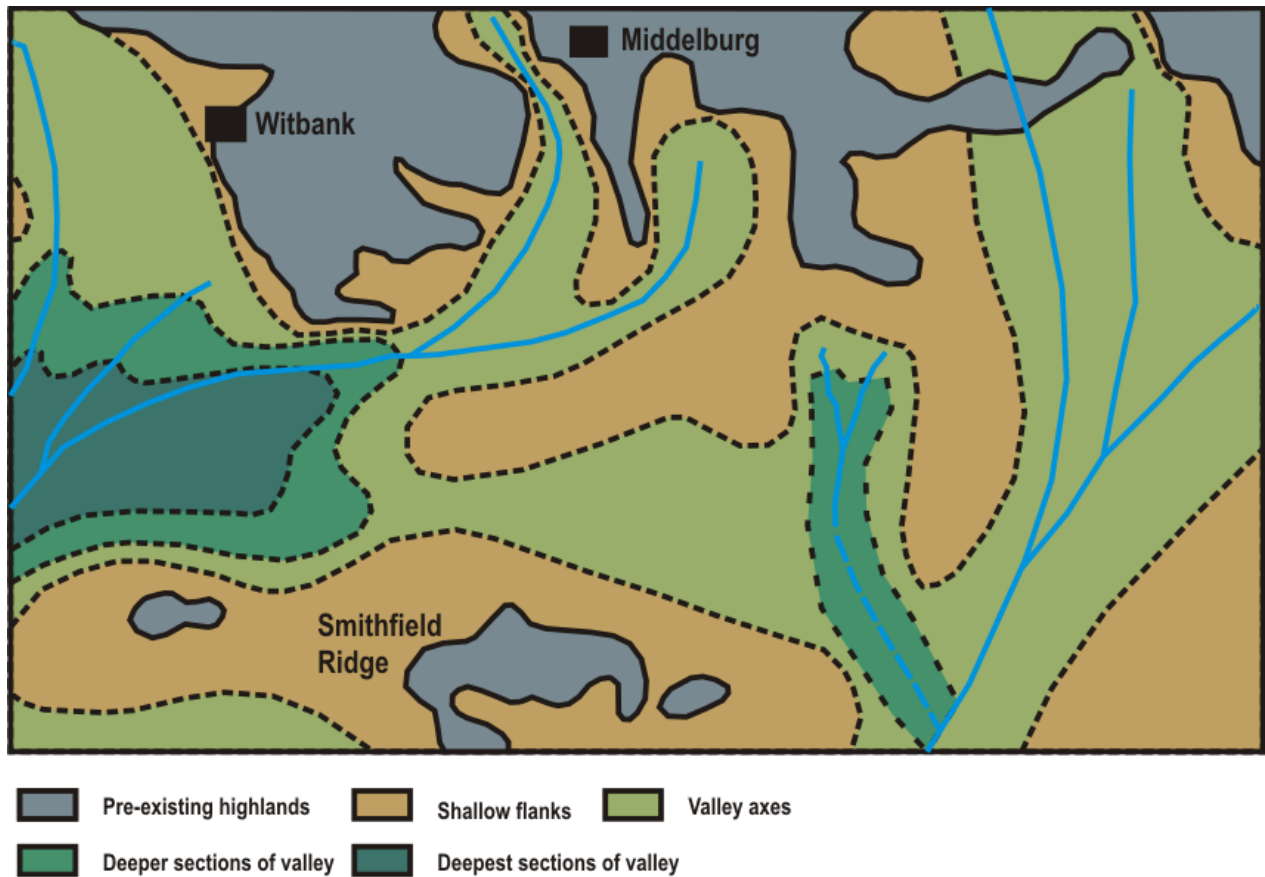


Figure 5.1: Palaeotopographic reconstruction of the central Witbank Coalfield and possible routes of river channels (adapted from Falcon, 1989).

5.2 Vegetation

5.2.1 Lower Coal Seam

The vegetation present in the Lower Coal Seam is controlled by the palaeoclimate as well as the local environment. The swamp-dominated environment is characteristic of the Lower Coal Seam, even when no intraseam parting is present. In the lowland areas, the abundance of both monoletate and trilete spores (observed genera include *Microbaculispora*, *Calamospora* and *Punctatisporites*) at all localities (Fig 4.1; 4.4; 4.7; 4.10; 4.13; 4.16) suggests a dominance of ferns, horsetail ferns and lycopods (Anderson, 1977). The highest spore abundances are found at localities HWH1418, BHS14 and sample 2 of ALBN11. The dominant presence of monosaccate pollen grains, especially in the lowest parts of the coal seam, is typical of post-glacial floras. Large monosaccate pollen grains are interpreted as belonging to the genus *Potonieisporites*, which has an affinity to the conifer genus *Walchia* in the Northern Hemisphere (Falcon, 1986). As noted by Falcon (1986), the lack of macrofossil evidence as well as conifers preference for drier areas suggest that they would occupy the uplands, away from the wetlands in the south. They may have also been present on the Smithfield Ridge. A *Florinites*-type monosaccate pollen grain, which features a trilete mark, was identified in the Lower Coal Seam only at localities BHS14, HWH1418 and S542145. This pollen grain is likely the Early Permian genus *Cannanoropollis*, a common species in other Gondwanan localities (Cazzulo-Klepzig *et al.*, 2009). This genus bears an affinity to *Cordaites*. *Cordaites* macrofossils have only been seen rarely in the Vryheid Formation near the base of the formation (Seward & Leslie, 1908). *Cordaites* is not a dominant plant in swamps but mangrove-like forms have been observed (Traverse, 2007), which suggests it is able to occupy wetter areas than conifers are able to, allowing it to find a specific ecological niche. Thus, *Cordaites* likely occupies the broad floodplains to the north of larger swamp and lake areas as it prefers wetter conditions to the conifers but is unable to grow well in the deeper swamps to the south. The low abundances of monosaccate pollen grains in the Lower Coal Seam of the southernmost locality S542145 also suggest that the coniferous monosaccate-producers are mainly present in the upland areas, with only a very small concentration of their pollen reaching the lowlands further away.

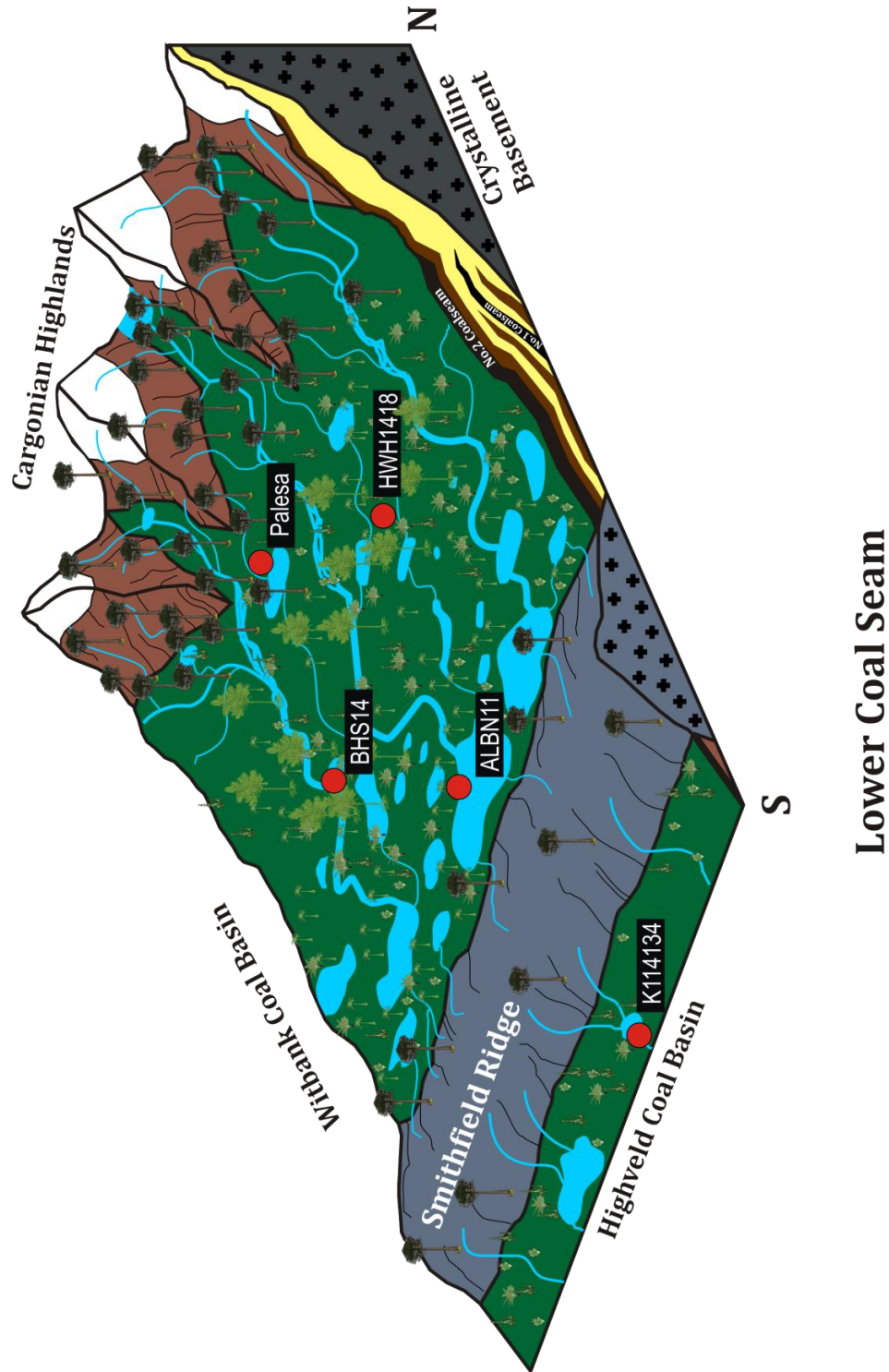


Figure 5.2: Model of the environment and vegetation of the Lower Coal Seam of the Witbank Coalfield and adjacent Highveld Coalfield. Small plants represent ferns, horsetail ferns and lycopods. Light green trees represent *Cordaites* flora. Dark green trees represent upland conifers. Red markers indicate studied localities.

5.2.2 Upper Coal Seam

The lowland areas of the Upper Coal Seam undergo shifts in environment which would in turn reflect the vegetation. The spore:pollen ratios in general are low in this seam (Fig. 4.6; 4.9; 4.15) with slight increases in the Palesa (Fig. 4.3) and ALBN11 (Fig. 4.12) localities when there is a switch to a swamp-dominated environment. This is documented in a switch from the fern-dominated lowland one sees in the Lower Coal Seam to a more varied but tree-dominated vegetation which can include ferns, horsetail ferns, cycads and larger glossopterid trees. *Glossopteris*, which are associated with taeniate bisaccate pollen grains, and *Gangamopteris*, which is associated with some of the non-taeniate bisaccate pollen grains (Falcon, 1986), would be mainly abundant on the broad swamps and floodplains. The low abundance of taeniate bisaccate pollen grains at the Palesa locality and very low abundance at the ALBN11 locality suggests a wet swampland which doesn't support the growth of large trees. In the uplands, glacial retreat based on the changing climate created conditions which support a greater diversity of gymnosperms. The non-taeniate bisaccate pollen genus *Pityosporites* and the taeniate pollen genus *Lueckisporites* are associated with different conifer species (Potonié & Kremp, 1956, Clement-Westerhof, 1974), and would be present in the drier uplands. At the southernmost locality S542145, the high but decreasing abundance of spores in the Upper Coal Seam (Fig. 4.16) initially suggests a marshland which supports both glossopterid trees and a diverse flora of fern, horsetail ferns and cycads with the trees becoming more dominant over time.

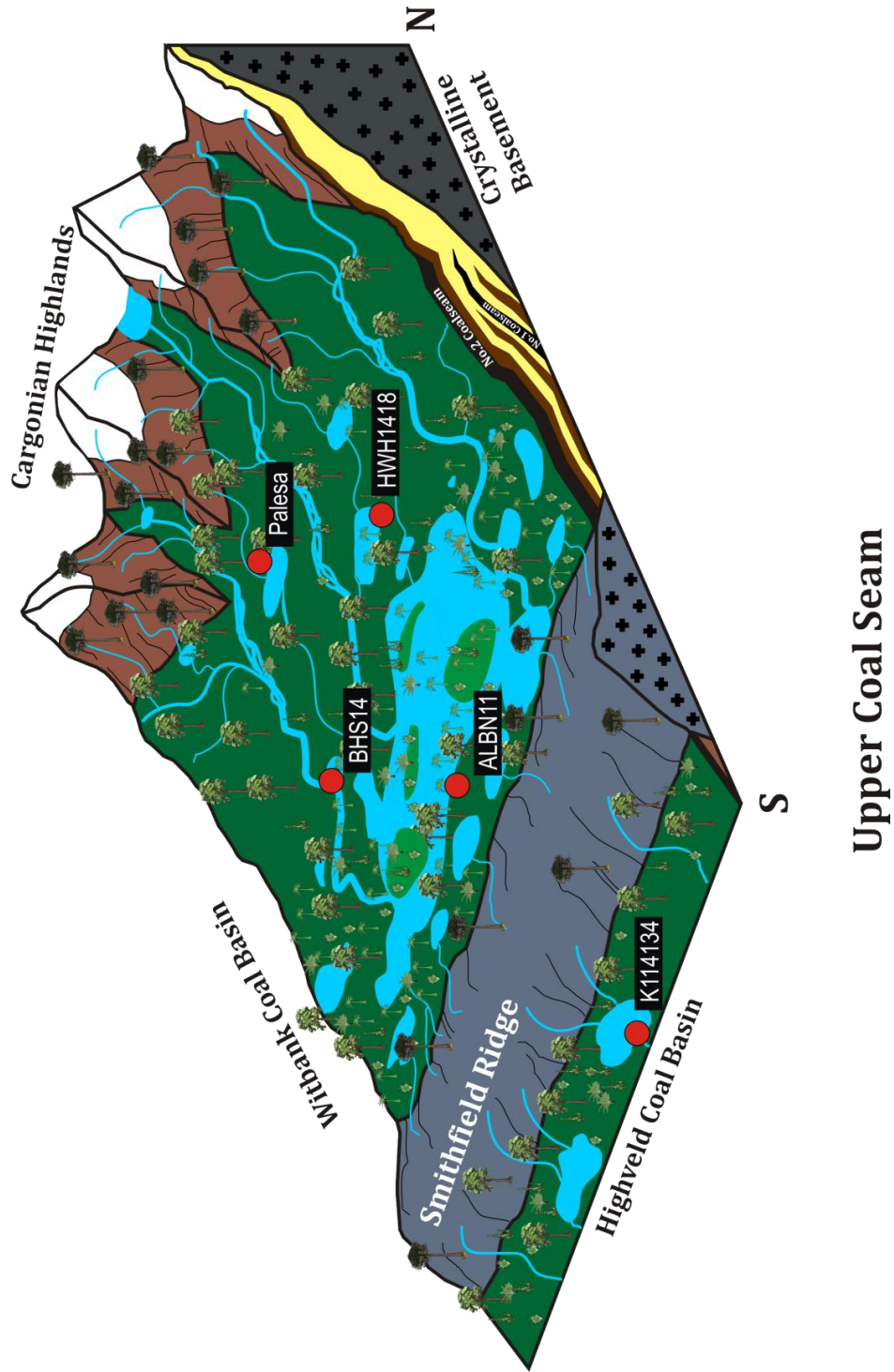


Figure 5.3: Model of the environment and vegetation of the Upper Coal Seam of the Witbank Coalfield and adjacent Highveld Coalfield. Small plants represent cycads, ferns and horsetail ferns. Light green trees represent Glossopterid flora. Dark green trees represent upland gymnosperms. Red markers indicate studied localities.

5.3 Palaeoclimate Analysis

Within the No. 2 Coal Seam of the Witbank and Highveld coalfields a clear trend of decreasing abundances of monosaccate pollen grains, coupled with an increase of bisaccate pollen grains and the appearance of taeniate pollen grains is seen at every locality studied (Plate 1, 2). This is clearly a regional occurrence based on a change in climate rather than a feature of local environment. The same trend is reported by Götz & Ruckwied (2014) and Ruckwied *et al.* (2014) from the No. 2 Coal Seam of the Inyanda Mine (Witbank), and confirms the potential of using climate signatures recorded in palynomorph assemblages for high-resolution cross basin correlation.

The monosaccate-producing vegetation is associated with the end of the Carboniferous Dwyka glaciation and is dominant in the No. 1 Coal Seam (Falcon, 1984). In the Upper No. 2 Coal Seam, the monosaccate-producing vegetation is replaced by the bisaccate-producing vegetation which becomes dominant in the early to mid-Permian (Falcon, 1984). This plant community indicates a cool-temperate climate with distinct seasonality and forces fern species into more restricted areas which remain permanently wet. Small-scale pulses of cooling can be seen when the environment shifts back to a swamp-dominated environment and the fern-dominated floral community proliferates in the deeper swamps (Fig. 4.12; 4.18) and valleys (Fig. 4.3).

The switch from a monosaccate-producing to a bisaccate- and striate-producing flora is also seen in other parts of Gondwana. Post-glacial floral shifts in the early-mid Permian are reported from southern Africa (D'Engelbronner, 1996; Modie & Le Herisse, 2009; Nyambe & Utting, 1997), Tanzania (Manum & Tien, 1973), Australia (Backhouse, 1991; Wopfner, 1999), Brazil (Cazzulo-Klepzig *et al.*, 2009; Iannuzzi *et al.*, 2010) and Oman (Stephenson *et al.*, 2005). This shift in floral composition in locations across Gondwana indicates a continent-wide change in climate. The likeliest reason for this is the northward movement of the continent across the equator with the margin of the Karoo Basin moving from 80°S in the late Carboniferous/early Permian to 40°S in the late Triassic/early Jurassic (Visser, 1986).

5.4 Comparison of Lower and Upper Coal Seams

In parts of the Witbank and Highveld coalfields, the Lower and Upper Coal Seams can be distinguished using a sandstone/siltstone marker bed (Cairncross and Cadle, 1988). But this marker bed is not present throughout all parts of the coalfields (Fig. 2.7), which makes correlation more difficult. In this study, localities with a clear intraseam parting (HWH1418, ALBN11, K114134, S542145) show distinct differences in the palynofacies of the Lower and the Upper coals seams. The major differences are related to the vegetation and climate. The pollen grain assemblages of the Lower Coal Seam are generally monosaccate-dominated while the Upper Coal Seam is generally bisaccate-dominated (Plate 1, 2). The spore:pollen ratios are generally high in the Lower Coal Seam except at locality ALBN11, and fluctuate or stay low in the Upper Coal Seam but this is dependent on the local palaeoenvironment. In general, the vegetation of the Lower Coal Seam reflects the cold climate of the Carboniferous/Permian interval with conifers dominating the upland and ferns dominating the lowland. The vegetation of the Upper Coal Seam reflects the fluctuating cool-temperate climate with more diverse, adaptable species like *Glossopteris*.

5.5 Comparison of Witbank and Highveld Coalfields

The major factor which differentiates the Witbank and Highveld coalfields is their position relative to the highlands to the north and the coastline to the south and the pre-Karoo topography which controls the depositional processes. The Witbank Coalfield in the north receives input of organic matter and sediments from meltwater outwash as glaciers receded in the early Permian (Cadle *et al.*, 1993). The variable nature of coal deposition in the Witbank Coalfield is due to the complex topography in the region. Deposition occurred in five recognized palaeovalleys (HWH1418, BHS14)(Fig. 6.3), across broader plains to the south (ALBN11) and in isolated valleys in the far north (Palesa) (Hancox & Götze, 2014). The Witbank Coalfield is bounded by the Cargonian Highlands and Smithfield Ridge which isolates the basin from the rest of the Main Karoo Basin. The palynofacies data supports the interpretation of a Gilbert-type lacustrine delta with coarse sedimentary material being supplied from the highlands.

Palaeocurrent analysis indicates the majority of sedimentary matter is transported into the basin from the north (Ryan, 1968). The sandstone parting at the HWH1418 and ALBN11 localities and the abundance of cuticles and larger plant debris (Plate 1) support the interpretation of a more proximal depositional environment. Streams running down from the highlands merge in the valleys to form either braided streams or meandering rivers. Large meandering rivers control sedimentation across the broad plains to the south. The rivers are blocked from moving further south by the Smithfield ridge which causes them to pond into wide, shallow swamps or lakes. These lakes were likely small and shallow as there is no evidence of black shale deposition like those seen in early Permian post-glacial lacustrine environments in East Africa (Kreuser & Woldu, 2010).

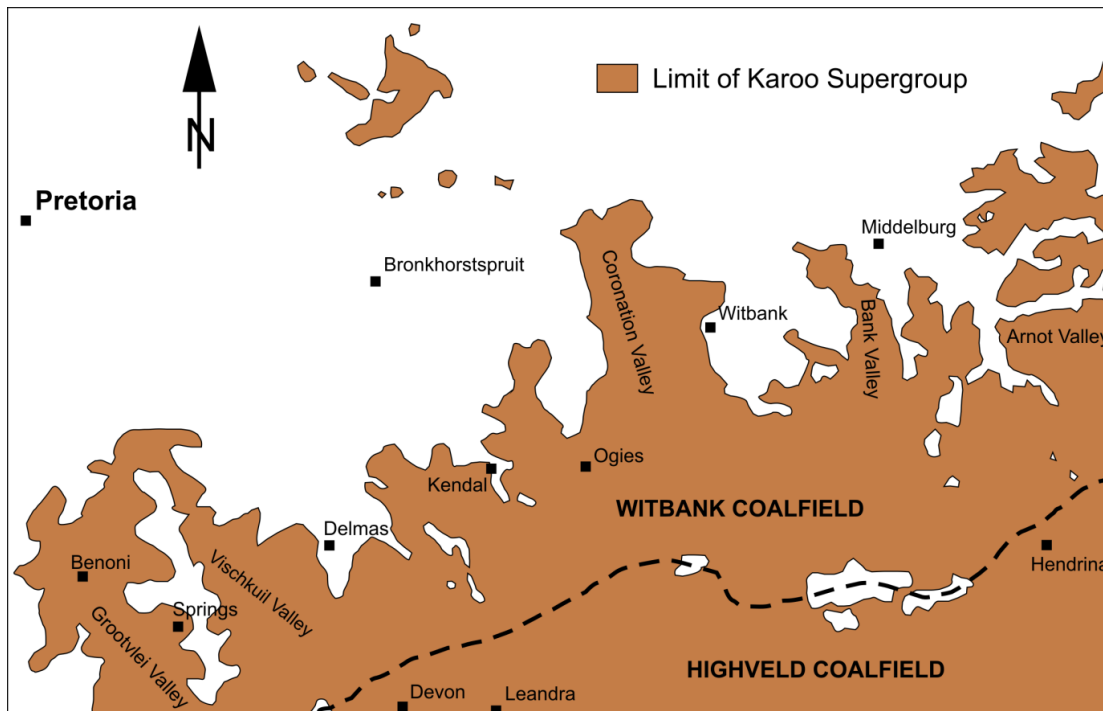


Figure 5.4: Map of the five major valleys in the Witbank Coalfield (from Hancox & Götz, 2014).

Previous work in the Highveld Coalfield noted the uneven palaeotopography which resulted in the irregular distribution of the coal (Van Vuuren & Cole, 1979) and a palaeoslope oriented to the south and south-east (Hagelskamp *et al.*, 1988). Deposition of sediments would have occurred on the broad plains south of the Smithfield Ridge (K114134) and into the two major north-south trending palaeovalleys which have been inferred for the Highveld Coalfield

(Hagelskamp *et al.*, 1988). One of these is a continuation of the Vischkuil Valley which begins in the Witbank Coalfield (S542145) (Hancox & Götz, 2014). Palaeocurrent analysis indicates that sediments are sourced mainly from the east and north-east with fewer channels coming out from the Witbank Coalfield (Ryan, 1968). The presence of a siltstone rather than a sandstone intraseam parting at both Highveld Coalfield localities and the smaller plant debris (Plate 2) suggest a more distal depositional environment. The results support the interpretation of extensive river-dominated delta plains. This interpretation agrees with the findings of Cadle & Hobday (1977) who proposed three major phases of sedimentation in the Highveld Coalfield: a lower deltaic-dominated phase, a river-dominated phase in which coal deposition occurs and an upper deltaic phase.

6. Conclusions

Palynofacies analysis of the No. 2 Coal Seam of 4 localities in the Witbank Coalfield and 2 localities in the Highveld Coalfield detail a regional shift in pollen-producing flora from monosaccate-dominated in the Lower Coal Seam to bisaccate-dominated in the Upper Coal Seam coinciding with the appearance of striate bisaccate pollen. This represents a climatic shift from a post-glacial cold to a fluctuating cool-temperate climate as a result of the northward movement of Gondwana during the Permian.

The palynological data also highlights shifts in the vegetational composition in the highlands and lowlands and the relationship of certain floral compositions with specific palaeoenvironments. The dry highland vegetation shifts from coniferous in the Lower Coal Seam to a more diverse gymnosperm- and pteridosperm-dominated community. The lowland vegetation of the Lower Coal Seam is dominated by ferns but includes horsetail ferns and lycopods as well as cordaitalean trees which may be limited to the palaeovalleys at the edge of the broad swamplands. In the Upper Coal Seam, *Glossopteris-Gangamopteris* vegetation becomes dominant along with a diverse community of cycads, ferns, lycopods and seed ferns.

Palaeoenvironmental analysis indicates a stable Lower Coal Seam which was mainly swamp-dominated. The sandstone intraseam parting in Witbank Coalfield indicates a more proximal environment while the siltstone parting in the Highveld Coalfield indicates a more distal environment. The palaeoenvironment of the Upper Coal Seam varies at each locality and is likely controlled by the warmer climate stimulating input of fresh meltwater from the regressing glaciers in the highlands and the uneven palaeotopography.

The palynological data of this study generally agrees with previous studies done in the area (Falcon, 1984; Götz & Ruckwied, 2014; Ruckwied *et al.*, 2014) but highlights the effect of the complex palaeotopography on the local environment and local floral composition. This study also provides first results of palynological research on the No. 2 Coal Seam of the Highveld Coalfield for comparison with the Witbank Coalfield.

7. Outlook

A major weakness of palynological research in Permian Gondwana is the tenuous nature of the botanical affinities of the observed pollen and spores. There is currently too much reliance on affinities inferred from Northern Hemisphere species. Combined research by both palynologists and palaeobotanists will be essential to unravelling the diverse and evolving flora which populated Gondwana. In the Main Karoo Basin in particular, this will allow detailed analysis of the vegetation in relation to the palaeoenvironment using the Sporomorph EcoGroup Model proposed by Abbink (2001) (Fig. 8.1). This model will allow for definitive comparison of upland, lowland and river vegetation.

Further palynological research on the Highveld Coalfield is also required with sampling on localities further south towards the palaeocoastline as the marine influence becomes more dominant. On a much larger scale, future studies must focus on (1) interregional palynofacies patterns in coeval basins, (2) comparison of floral composition and shifts in coeval basins and (3) a palynostratigraphic framework for Gondwana-wide correlation.

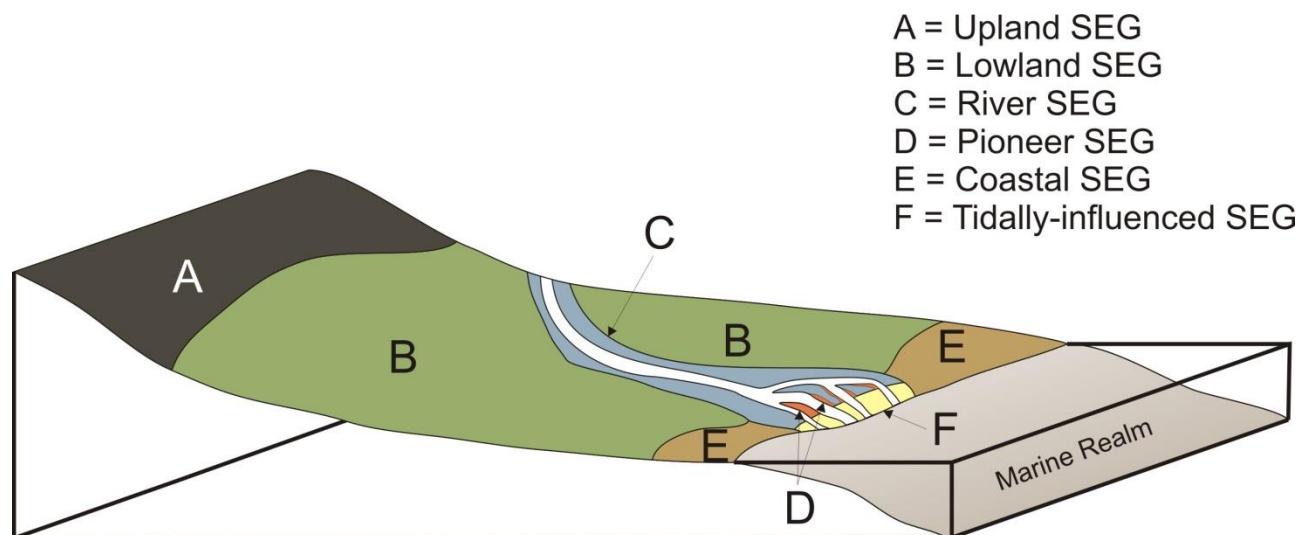


Figure 7.1: Schematic diagram of the Sporomorph EcoGroup Model. Plant species are grouped into different SEGs based on their habitat preferences which are controlled by the climate and environment (adapted from Abbink, 2001).

References

Abbink, O., Targarona, J., Brinkhuis, H., Visscher, H., 2001. Late Jurassic to earliest Cretaceous palaeoclimatic evolution of the southern North Sea. *Global and Planetary Change* 30(3): 231-256.

Aitken, G.A., 1993. Palynology of the Number Five Seam in the Witbank/Highveld coalfields. Unpublished M.Sc. Thesis, University of the Witwatersrand.

Aitken, G.A., 1994. Permian palynomorphs from the Number 5 Seam, Ecca Group, Witbank Highveld Coalfields, South Africa. *Palaeontologia africana* 31: 97-109.

Aitken, G.A., 1998. A palynological and palaeoenvironmental analysis of Permian and Early Triassic sediments of the Ecca and the Beaufort groups, Northern Karoo Basin, South Africa. Unpublished Ph.D. Thesis, University of the Witwatersrand.

Anderson, J.M., 1977. The biostratigraphy of the Permian and Triassic. Part 3. A review of Gondwana palynology with particular reference to the northern Karoo Basin, South Africa. *Memoirs of the Botanical Survey of South Africa* 4: 1-33.

Backhouse, J., 1991. Permian palynostratigraphy of the Collie Basin, western Australia. *Review of Palaeobotany and Palynology* 67(3): 237-314.

Backhouse, J., 1993. Palynology and correlation of Permian sediments in the Perth, Collie, and Officer basins, Western Australia. *Geological Survey Western Australia, Report 34*: 111-128.

Barbolini, N., 2010. Palynology of a coal seam in Karoo deposits of Botswana and correlation with southern African coal-bearing strata. Unpublished MSc Thesis, University of the Witwatersrand.

Barbolini, N., 2014. Palynostratigraphy of the South African Karoo Supergroup and correlations with coeval Gondwanan Successions. Unpublished PhD Thesis, University of the Witwatersrand.

Broom, R., 1906. V.—On the Permian and Triassic Faunas of South Africa. *Geological Magazine (Decade V)* 3(1): 29-30.

Cadle, A. B., Cairncross, B., Christie, A. D. M., Roberts, D. L., 1993. The Karoo Basin of South Africa: type basin for the coal-bearing deposits of southern Africa. *International Journal of Coal Geology* 23(1): 117-157.

Cadle, A. B., Hobday, D. K., 1977. A subsurface investigation of the Middle Ecca and Lower Beaufort in northern Natal and the southeastern Transvaal. *Transactions Geological Society South Africa* 80: 111-117.

Cairncross, B., 1989. Paleodepositional environments and tectonosedimentary controls of the postglacial Permian coals, Karoo Basin, South Africa. *International Journal of Coal Geology* 12(1): 365-380.

Cairncross, B., Cadle, A. B., 1988. Palaeoenvironmental control on coal formation, distribution and quality in the Permian Vryheid Formation, East Witbank Coalfield, South Africa. *International Journal of Coal Geology* 9: 343-370.

Catuneanu, O., 2002. Sequence stratigraphy of clastic systems: concepts, merits, and pitfalls. *Journal of African Earth Sciences* 35(1): 1-43.

Catuneanu, O., Hancox, P. J., Rubidge, B. S., 1998. Reciprocal flexural behaviour and contrasting stratigraphies: a new basin development model for the Karoo retroarc foreland system, South Africa. *Basin Research* 10(4): 417-439.

Catuneanu, O., Wopfner, H., Eriksson, P.G., Cairncross, B., Rubidge, B.S., Smith, R.M.H., Hancox, P.J., 2005. The Karoo basins of south-central Africa. *Journal of African Earth Sciences* 43: 211–253.

Cazzulo-Klepzig, M., Mendonça Filho, J. G., Guerra-Sommer, M., Menezes, T. R., Simas, M. W., Mendonca, J. O., Degani-Schmidt, I., 2009. Effect of volcanic ash-fall on a Permian peat-forming environment, on the basis of palynology, palynofacies and paleobotany (Faxinal Coalfield, Brazil). *Revista Brasileira de Paleontologia* 12(3): 179-194.

Clement-Westerhof, J. A., 1974. In situ pollen from gymnospermous cones from the Upper Permian of the Italian Alps—a preliminary account. *Review of Palaeobotany and Palynology* 17(1): 63-73.

d'Engelbronner, E. R., 1996. New palynological data from Karoo sediments, Mana Pools basin, northern Zimbabwe. *Journal of African Earth Sciences* 23(1): 17-30.

Department of Mineral and Energy Affairs. 2628 East Rand [map]. Edition. 1:250 000. Pretoria: The Government Printer, 1986.

Department of Mines. 2528 Pretoria [map]. Edition. 1:250 000. Pretoria: The Government Printer, 1978.

Eskom, 2015. Website: www.eskom.co.za. Last Accessed: 22 September 2015.

Falcon, R.M.S., Pinheiro, H.J., Sheperd, P., 1984. The palynostratigraphy of the major coal seams in the Witbank Basin with lithostratigraphic, chronostratigraphic and palaeoclimatic implications. *Communicacoes Servicos Geológicos Portugal* 70: 215–243.

Falcon, R.M.S., 1986. A brief review of the origin, formation and distribution of coal in Southern Africa. *Mineral Deposits of Southern Africa* 2: 1879-1898.

Falcon, R. M. S., 1989. Macro-and micro-factors affecting coal-seam quality and distribution in southern Africa with particular reference to the No. 2 seam, Witbank coalfield, South Africa. *International Journal of Coal Geology* 12(1): 681-731.

Flint, S., Hodgson, D., Sprague, A., Brunt, R., Van der Merwe, W., Figueiredo, J., Pr lat, A., Box, D., Di Celma, C., Kavanagh, J., 2010. Depositional architecture and sequence stratigraphy of the Karoo basin floor to shelf edge succession, Laingsburg depocentre, South Africa. *Marine and Petroleum Geology* 28(3): 658-674.

Fourie, C. J. S., Henry, G., Mare, L. P., 2014. The Structure of the Karoo-age Ellisras Basin in Limpopo Province, South Africa, in the light of New Airbourne Geophysical Data. *South African Journal of Geology* 117(2): 193-210.

Gastaldo, R.A. 1994. The genesis and sedimentation of phytoclasts with examples from coastal environments In: A. Traverse (ed.) Sedimentation of organic particles, Cambridge University Press, p. 103-127.

G tz, A.E., Ruckwied, K., Littke, R., Hartkopf-Fr der, C., 2012. Facies, sedimentary organic matter content and coal petrography of the No. 2 coal seam, northern Witbank Basin (South Africa). - Proceedings of the 34th International Geological Congress 2012, Abstract 3383 (CD-ROM, ISBN 978-0-646-57800-2); Brisbane.

G tz, A.E., Ruckwied, K., 2014. Palynological records of the Early Permian postglacial climate amelioration (Karoo Basin, South Africa). *Palaeobiodiversity and Palaeoenvironments* 94(2): 229–235.

Hagelskamp, H. H. B., Eriksson, P. G., Snyman, C. P. 1988. The effect of depositional environment on coal distribution and quality parameters in a portion of the Highveld Coalfield, South Africa. *International journal of coal geology* 10(1): 51-77.

Hancox, J.P., Götz, A.E., 2014. South Africa's coalfields – a 2014 perspective. *International Journal of Coal Geology* 132: 170–254.

Hart, G.F., 1967. Micropalaeontology of the Karroo deposits in South and Central Africa. In: I.U.G.S. Secretariat, Ed., *Reviews/or the first symposium on Gondwana stratigraphy*, Haarlem, Netherlands: 161-172.

Hodgson, D.M., Flint, S., Drinkwater, N.J., Johannesson, E.P., Luthi, S., 2006. Palaeogeographic and stratigraphic evolution of submarine fan systems in the Tanqua depocentre South Africa. *Journal of Sedimentary Research* 76: 19-39.

Iannuzzi, R., Souza, P. A., Holz, M., 2010. Stratigraphic and paleofloristic record of the Lower Permian postglacial succession in the southern Brazilian Paraná Basin. *Geological Society of America Special Papers* 468: 113-132.

Isbell, J. L., Cole, D. I., Catuneanu, O., 2008. Carboniferous-Permian glaciation in the main Karoo Basin, South Africa: Stratigraphy, depositional controls, and glacial dynamics. *Geological Society of America Special Papers* 441: 71-82.

Johnson, M.R., Van Vuuren, C.J., Hegenberger, W.F., Key, R., Shoko, U., 1996. Stratigraphy of the Karoo Supergroup in southern Africa: an overview. *Journal of African Earth Sciences* 23(1): 3-15.

Johnson, M. R., Van Vuuren, C. J., Visser, J. N. J., Cole, D. I., Wickens, H. D. V., Christie, A. D. M., Roberts, D. L., 1997. The foreland Karoo Basin, South Africa. African basins. *Sedimentary basins of the World* 3: 269-317.

Johnson, S. D., Flint, S. S., Hinds, D., Wickens, H. D. V., 2001. Anatomy of basin floor to slope turbidite systems, Tanqua Karoo, South Africa: sedimentology, sequence stratigraphy and implications for subsurface prediction. *Sedimentology* 48: 987-1023.

Kreuser, T., Woldu, G., 2010. Formation of euxinic lakes during the deglaciation phase in the Early Permian of East Africa. *Geological Society of America Special Papers* 468: 101-112.

MacRae, C.S., 1988. Palynostratigraphic correlation between the Lower Karoo sequence of the Waterberg and Pafuri coal-bearing basins and the Hammanskraal plant macrofossil locality, Republic of South Africa. *Memoirs Geological Survey of South Africa* 75: 1–217.

MacRae, C. S., Aitken, G. A., 1997. Contributions in the field of palaeopalynology at the Bernard Price Institute, past, present and future. *Palaeontologia Africana* 33: 37-40.

Manum, S. B., Tien, N. D., 1973. Palyno-stratigraphy of the Ketewaka Coalfield (Lower Permian), Tanzania. *Review of Palaeobotany and Palynology* 16(4): 213-227.

McKay, M. P., Weislogel, A. L., Fildani, A., Brunt, R. L., Hodgson, D. M., & Flint, S. S., 2015. U-PB zircon tuff geochronology from the Karoo Basin, South Africa: implications of zircon recycling on stratigraphic age controls. *International Geology Review* 57(4): 393-410.

Millstead, B.D., 1994. Palynological evidence for the age of the Permian Karoo coal deposits near Vereeniging, northern Orange Free State, South Africa. *South Africa Journal of Geology* 97(1): 15-20.

Millstead, B.D., 1999. Palynology of the Early Permian coal-bearing deposits near Vereeniging, Free State, South Africa. *Bulletin of the Geological Survey of South Africa* 124: 1–77.

Modie, B. N., Le Hérisse, A., 2009. Late Palaeozoic palynomorph assemblages from the Karoo Supergroup and their potential for biostratigraphic correlation, Kalahari Karoo Basin, Botswana. *Bulletin of Geosciences* 84(2): 337-358.

Nyambe, I. A., Utting, J., 1997. Stratigraphy and palynostratigraphy, Karoo Supergroup (Permian and Triassic), mid-Zambezi Valley, southern Zambia. *Journal of African Earth Sciences* 24(4): 563-583.

Potonié, R., Kremp, G., 1956. Die Sporaee Dispersae des Ruhrkarbons, ihre Morphographie und Stratigraphie mit Ausblicken auf Arten anderer Gebiete und Zeitabschnitte. Teil II. *Palaeontographica Abteilung B*: 85-191.

Powell, A. J., Dodge, J. D., Lewis, J., 1990. Late Neogene to Pleistocene Palynological Facies of the Peruvian Continental Margin Upwelling, LEG 1121.

Rubidge, B.S., Johnson, M.R., Kitching, J.W., Smith, R.M.H., Keyser, A.W., Groenewald, G.H., 1995. An introduction to the biozonation of the Beaufort Group. In: Rubidge, B.S. (Ed.), *Reptilian Biostratigraphy of the Permian–Triassic Beaufort Group (Karoo Supergroup): SACS Biostratigraphic Series 1*: 1-2.

Rubidge, B. S., Erwin, D. H., Ramezani, J., Bowring, S. A., de Klerk, W. J., 2013. High-precision temporal calibration of Late Permian vertebrate biostratigraphy: U-Pb zircon constraints from the Karoo Supergroup, South Africa. *Geology* 41(3): 363-366.

Ruckwied, K., Götz, A.E., Jones, P., 2014. Palynological records of the Permian Ecca Group (South Africa): Utilizing climatic icehouse–greenhouse signals for cross basin correlations. *Palaeogeography, Palaeoclimatology, Palaeoecology* 413: 167–172.

Ryan, P. J., 1968. Stratigraphy of the Ecca Series and Lowermost Beds (Permian) in the Great Karoo Basin of South Africa. *Unpublished Ph. D. Thesis, Univ. Witwatersrand, Johannesburg. Nieman.*

Seward, A.C., Leslie, T. N., 1908. Permo-Carboniferous Plants from Vereeniging, Transvaal. *Quarterly Journal of the Geological Society* 64(1-4): 109-126.

Snyman, C. P., 1998. Coal. *The Mineral Resources of South Africa. Handbook 16*: 136-205.

Stephenson, M. H., Leng, M. J., Vane, C. H., Osterloff, P. L., Arrowsmith, C., 2005. Investigating the record of Permian climate change from argillaceous sedimentary rocks, Oman. *Journal of the Geological Society* 162(4): 641-651.

Stephenson, M. H., 2008. Spores and pollen from the middle and upper Gharif members (Permian) of Oman. *Palynology* 32(1): 157-182.

Stephenson, M. H., & McLean, D., 1999. International correlation of Early Permian palynofloras from the Karoo sediments of Morupule, Botswana. *South African Journal of Geology* 102(1): 3-14.

Traverse, A., 2007. *Paleopalynology, Second Edition (Topics in Geobiology 28)*. Springer, Dordrecht, Netherlands.

Tyson, R. V., 1995. *Sedimentary organic matter: organic facies and palynofacies*. Chapman and Hall. London. New York.

Van Vuuren, C. J., Cole, D. I., 1979. The stratigraphy and depositional environments of the Ecca Group in the northern part of the Karoo Basin. In: *Some Sedimentary Basins and Associated Ore Deposits of South Africa* 6: 103-111.

Vidal, G., 1988. A palynological preparation method. *Palynology* 12: 215-220.

Visser, J. N. J., 1986. Lateral lithofacies relationships in the glaciogene Dwyka Formation in the western and central parts of the Karoo Basin. *Transactions of the Geological Society of South Africa* 89: 373-383.

Wopfner, H., 1999. The early Permian deglaciation event between East Africa and northwestern Australia. *Journal of African Earth Sciences* 29(1): 77-90.

Appendices

Palynofacies Counting Sheets

Palesa

Palynofacies	Sample No.	1	2	3	4	5	6	7	8	9	10
Phytoclasts	opaque equidimensional	268	285	280	279	158	276	238	126	102	110
	opaque needle-shaped	76	83	70	65	36	45	56	10	15	12
	translucent equidimensional	28	18	17	10	148	18	15	175	185	161
	translucent needle-shaped	13	5	6	6	32	8	3	14	24	28
	cuticles and bigger plant debris	9	4	3	3	1	5	8	2	1	1
Palynomorphs	<i>Pollen grains</i>										
	monosaccate	35	42	38	45	21	10	25	12	4	0
	bisaccate, non-taeniate	26	21	33	38	53	68	80	72	68	85
	bisaccate, taeniate	0	0	0	1	10	37	42	56	58	65
	<i>Spores</i>										
	monolete	2	4	1	1	0	0	0	0	0	0
	trilete	12	10	18	14	1	8	9	1	1	1
Other	Amorphous Organic Matter (AOM)	12	16	15	19	2	12	15	1	2	1
	Degraded Organic Matter (DOM)	20	15	24	22	30	20	18	32	35	30
Algae		0	0	0	0	9	0	0	6	10	8
Total		501	503	505	503	501	507	509	507	505	502

HWH1418

Palynofacies	Sample No.	1	2	3	4	5	6	7	8	9	10	11	12	13	14
Phytoclasts	opaque equidimensional	265	251	271	276	343	363	335	153	143	150	138	125	110	121
	opaque needle-shaped	50	69	58	60	28	24	15	84	57	50	42	65	70	19
	translucent equidimensional	53	46	35	39	24	20	31	168	152	177	186	162	165	190
	translucent needle-shaped	24	21	28	17	8	10	10	35	43	28	35	52	38	37
	cuticles and bigger plant debris	8	12	5	8	1	0	1	2	5	1	7	5	1	1
Palynomorphs	<i>Pollen grains</i>														
	monosaccate	10	15	11	7	8	5	5	1	3	1	1	0	0	0
	bisaccate, non-taeniate	10	7	13	10	20	18	27	20	37	45	31	47	55	63
	bisaccate, taeniate	0	0	0	0	0	2	2	13	31	24	26	22	38	38
	<i>Spores</i>														
	monolete	10	6	3	5	1	2	2	0	0	1	1	1	0	0
	trilete	38	42	52	49	12	7	10	1	0	4	1	1	3	2
Other	Amorphous Organic Matter (AOM)	25	18	16	22	0	0	0	3	1	1	5	1	2	1
	Degraded Organic Matter (DOM)	10	15	9	12	58	52	67	18	25	16	20	21	15	23
Algae		0	0	0	0	1	0	1	9	5	12	9	6	10	11
Total		503	502	501	505	504	503	506	507	502	508	502	508	507	506

BHS14

Palynofacies	Sample No.	1	2	3	4	5	6	7	8	9	10
Phytoclasts	opaque equidimensional	209	211	225	200	248	207	150	238	241	200
	opaque needle-shaped	53	69	85	128	88	120	24	75	83	115
	translucent equidimensional	115	90	60	51	43	45	182	50	63	47
	translucent needle-shaped	38	25	19	24	26	30	53	20	12	18
	cuticles and bigger plant debris	12	8	7	8	5	8	1	6	9	10
Palynomorphs	<i>Pollen grains</i>										
	monosaccate	15	20	12	18	10	10	3	1	1	0
	bisaccate, non-taeniate	1	8	13	9	9	7	18	35	28	47
	bisaccate, taeniate	0	0	0	0	0	2	21	36	38	35
	<i>Spores</i>										
	monolete	7	4	8	10	10	5	0	1	0	0
	trilete	28	41	48	37	35	42	3	12	5	2
Other	Amorphous Organic Matter (AOM)	18	25	19	11	18	16	2	20	18	23
	Degraded Organic Matter (DOM)	12	10	6	8	15	12	38	7	8	8
Algae		0	0	0	0	0	0	11	0	0	0
Total		508	511	502	504	507	504	506	501	506	505

ALBN11

Palynofac	Sample no	1	2	3	4	5	6	7	8
Phytoclas	opaque ec	180	211	139	125	143	155	189	145
	opaque ne	48	52	49	29	36	44	46	37
	translucen	194	217	263	163	205	199	143	217
	translucen	54	52	79	58	55	53	46	72
	cuticles ar	3	2	1	7	1	2	1	1
Palynom	<i>Pollen grains</i>								
	monosacc	13	14	15	20	18	4	1	0
	bisaccate,	1	5	9	16	21	14	29	29
	bisaccate,	0	0	0	3	0	0	2	1
	<i>Spores</i>								
	monolete	6	0	2	8	11	4	0	7
	trilete	6	28	7	18	19	18	25	16
Other	Amorphou	0	0	0	5	1	1	3	0
	Degraded	13	10	19	52	19	8	16	13
Algae		0	0	0	0	0	0	0	0
Total		518	591	583	504	529	502	501	538

K114134

Palynofacies	Sample No.	1	2	3	4	5	6	7	8	9	10	11	12
	2L (1-4), 2U (8-12)												
Phytoclasts	opaque equidimensional	214	236	248	237	212	268	276	168	253	250	150	133
	opaque needle-shaped	46	30	28	42	58	4	6	40	35	31	38	25
	translucent equidimensional	143	129	109	95	97	98	90	178	83	86	173	185
	translucent needle-shaped	28	18	12	14	16	8	12	43	12	10	28	35
	cuticles and bigger plant debris	10	7	8	12	9	1	1	3	10	5	3	4
Palynomorphs	<i>Pollen grains</i>												
	monosaccate	14	17	15	20	18	25	21	12	7	9	3	0
	bisaccate, non-taeniate	2	7	9	13	24	18	23	28	42	52	58	67
	bisaccate, taeniate	0	0	0	0	0	3	4	12	23	27	31	35
	<i>Spores</i>												
	monolete	5	8	4	5	2	4	2	0	1	2	0	0
	trilete	28	32	43	38	40	8	10	0	12	7	1	1
Other	Amorphous Organic Matter (AOM)	8	12	15	11	15	0	1	3	13	15	2	2
	Degraded Organic Matter (DOM)	15	13	10	17	10	63	67	16	8	10	18	16
Algae		0	0	0	0	0	2	1	7	2	1	9	6
Total		513	509	501	504	501	502	514	510	501	505	514	509

S542145

Palynofacies	Sample No.	1	2	3	4	5	6	7	8
Phytoclasts	opaque equidimensional	214	175	93	235	159	185	138	155
	opaque needle-shaped	108	120	127	159	121	88	129	119
	translucent equidimensional	61	56	124	22	83	75	62	73
	translucent needle-shaped	32	48	88	18	41	48	23	32
	cuticles and bigger plant debris	10	3	8	0	15	3	8	12
Palynomorphs	<i>Pollen grains</i>								
	monosaccate	15	4	3	1	3	1	1	1
	bisaccate, non-taeniate	12	28	15	18	18	38	42	32
	bisaccate, taeniate	0	0	0	0	3	18	38	30
	<i>Spores</i>								
	monolete	21	23	22	12	30	28	34	18
	trilete	12	24	9	5	14	10	8	5
Other	Amorphous Organic Matter (AOM)	0	0	1	0	0	0	1	0
	Degraded Organic Matter (DOM)	22	23	13	31	22	12	17	25
Algae		0	0	2	0	0	0	0	0
Total		507	504	505	501	509	506	501	502

Plate 1: Palynofacies of Coal Seam No. 2, Witbank Coalfield

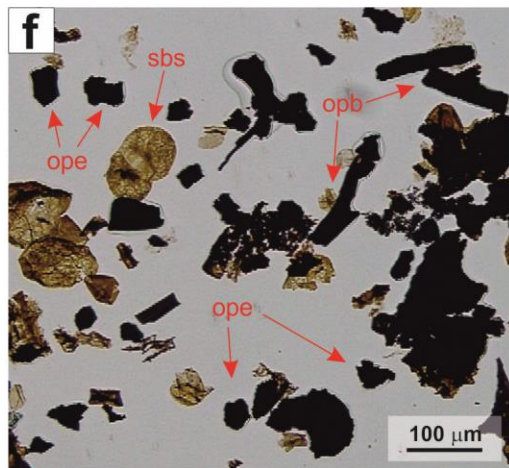
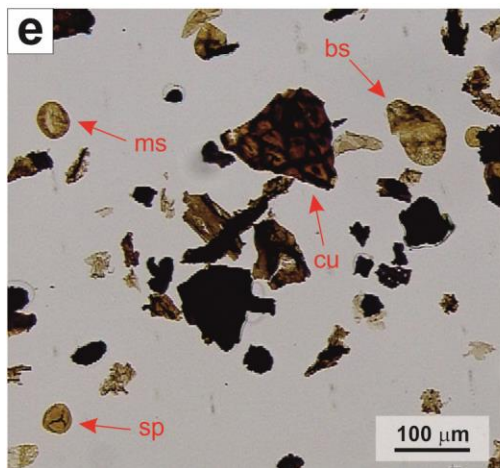
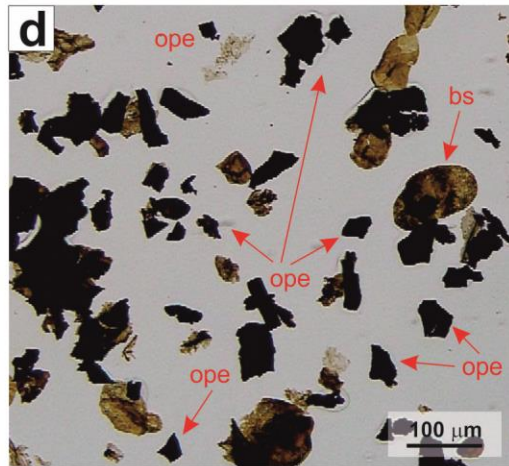
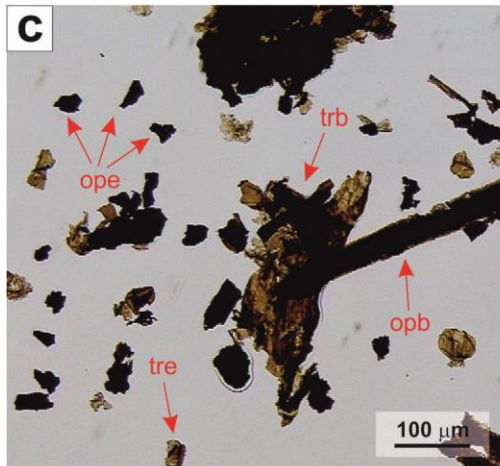
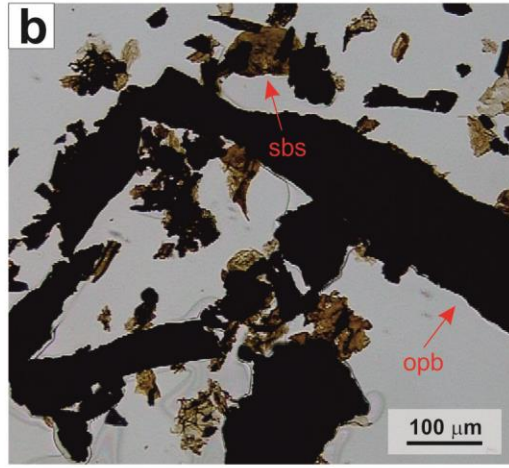
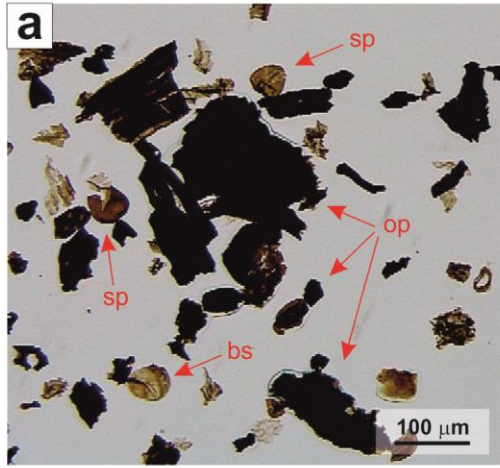


Plate 2: Palynofacies of Coal Seam No. 2, Highveld Coalfield

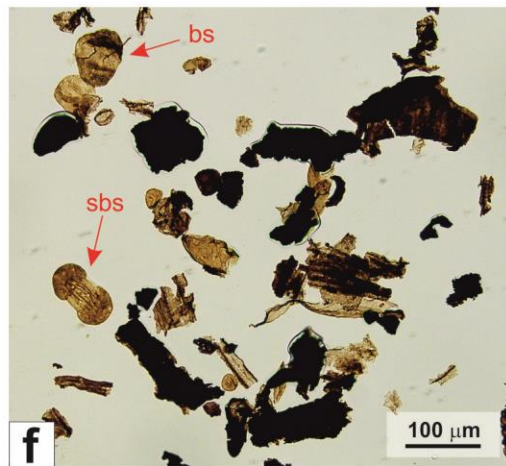
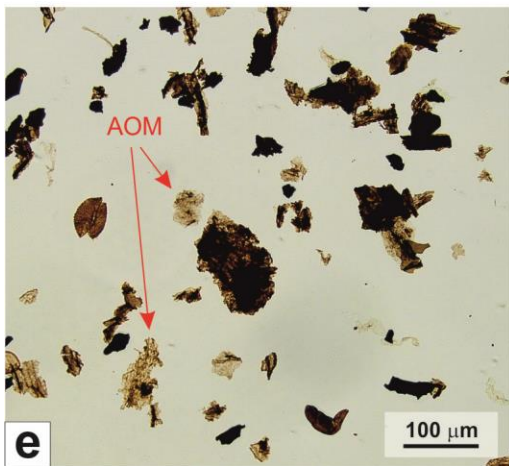
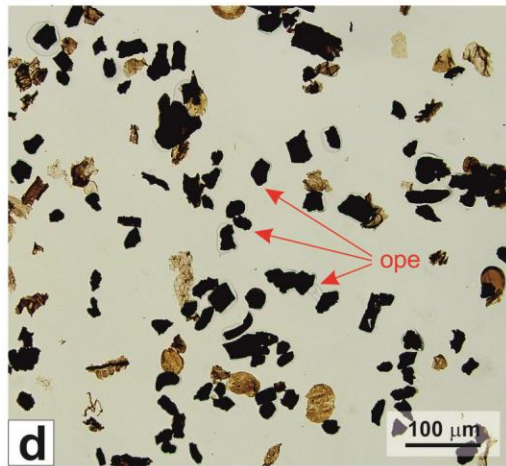
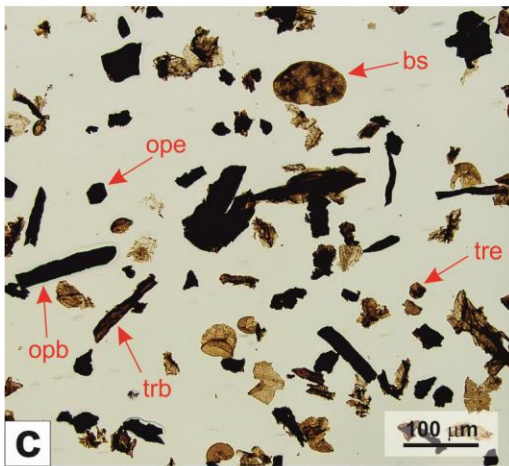
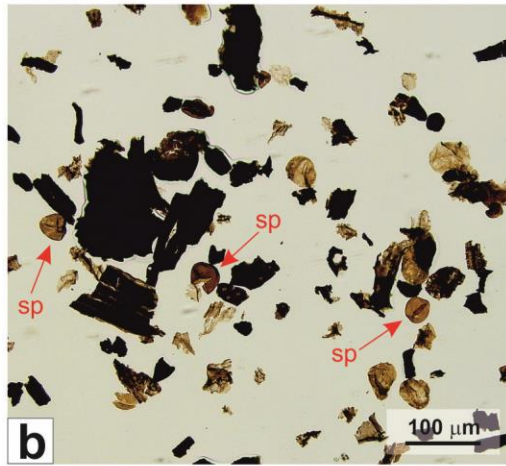
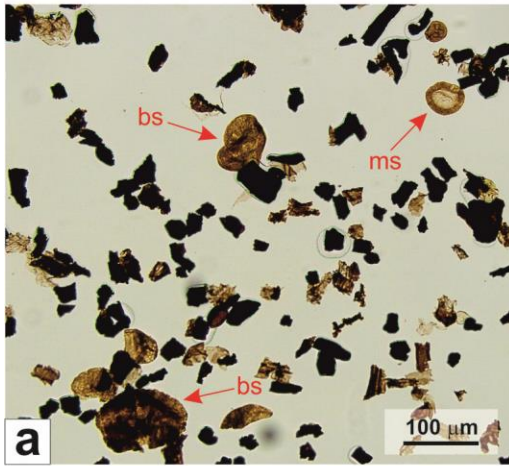


Plate 1: Palynofacies of Coal Seam No. 2, Witbank Coalfield

a: Lower Seam (HWH1418). High amount of opaque phytoclasts and spores. op = opaque phytoclast, sp = spore, bs = bisaccate pollen grain.

b: Upper Seam (BHS14). High amount of large, opaque blade-shaped phytoclasts and striate bisaccate pollen grains. opb = opaque blade-shaped phytoclast, sbs = striate bisaccate pollen grain.

c: Upper Seam, lake setting (Palesa). Phytoclasts of various sizes and shapes. ope = opaque equidimensional, opb = opaque blade-shaped, tre = translucent equidimensional, trb = translucent blade-shaped.

d: Intra seam, fluvial setting (ALBN11). High amount of opaque equidimensional phytoclasts. ope = opaque equidimensional phytoclast, bs = bisaccate pollen grain.

e: Lower Seam (BHS14). High amount of cuticles, spores, and pollen grains (monosaccate and bisaccate). bs = bisaccate pollen grain, ms = monosaccate pollen grain, cu = cuticle, sp = spore.

f: Upper Seam (BHS14). High amount of opaque phytoclasts and striate bisaccate pollen grains. ope = opaque equidimensional, opb = opaque blade-shaped, sbs = striate bisaccate pollen grain.

Plate 2: Palynofacies of Coal Seam No. 2, Highveld Coalfield

a: Lower Seam (S542145). High amount of monosaccate and bisaccate pollen grains. bs = bisaccate pollen grain, ms = monosaccate pollen grain.

b: Lower Seam, swamp setting (K114314). High amount of spores. sp = spore.

c: Lower Seam, lake setting (S542145). Phytoclasts of various sizes and shapes. ope = opaque equidimensional, opb = opaque blade-shaped, tre = translucent equidimensional, trb = translucent blade-shaped.

d: Intra seam, fluvial setting (K114314). High amount of opaque equidimensional phytoclasts. ope = opaque equidimensional.

e: Upper Seam, swamp setting (K114314). High amount of amorphous organic matter (AOM).

f: Upper Seam (S542145). High amount of bisaccate and striate bisaccate pollen grains. bs = bisaccate pollen grain, sbs = striate bisaccate pollen grain.